International Journal of Mathematical Archive-8(1), 2017, 161-189
Available online through www.ijma.info ISSN 2229 – 5046

COMBINED INFLUENCE OF THERMAL RADIATION, SORET, DUFOUR EFFECTS ON NON-DARCY MIXED CONVECTIVE HEAT AND MASS TRANSFER FLOW WITH DISSIPATIVE IN A VERTICAL CHANNEL

[1]R. BHUVANA VIJAYA, [2]B. HARITHA* AND [3]D. R. V. PRASADA RAO

[1]Department of Mathematics,
J. N. T. U. A Engineering College, Ananthapuramu -515001, (A.P.), India.

[2]Department of Mathematics,
Sri Krishnadevaraya University, Ananthapuramu -515003, (A.P.), India.

(Received On: 19-12-16; Revised & Accepted On: 11-01-17)

ABSTRACT

An attempt has been made to investigate the effect of dissipation and thermal radiation on convective heat and mass transfer in a vertical channel with Soret and Dufour effects using Galerkin finite element technique. The governing equations of flow heat and mass transfer have been solved to obtain Velocity, Temperature and Concentration. The effects of dissipation and thermal radiation on the flow characteristics have been investigated.

***Key Words**: Dissipation, Thermal Radiation, Non-Darcy flow, Finite element analysis.*

1. INTRODUCTION

The vertical channel is a frequently encountered configuration in thermal engineering equipment, for example, collectors of solar energy, cooling devices of electronic and Micro-electronic equipments etc. The influence of electrically conducting the case of fully developed mixed convection between horizontal parallel plates with a linear axial temperature distribution was solved by Gill and Casal [26]. Ostrach [42] solved the problem of fully developed mixed convection between vertical plates with and without heat sources. Cebeci *et al.* [14] performed numerical calculations of developing laminar mixed convection between vertical parallel pates for both cases of buoyancy aiding and opposing conditions. Wirtz and McKinley [64] conducted an experimental study of a opposing mixed convection between vertical parallel plates with one plate heated and the other adiabatic. Al-Nimir and Haddad [5] have described the fully developed free convection in an open-ended vertical channel partially filled with porous material. Greif *et al.* [27] have made an analysis on the laminar convection of a radiating gas in a vertical channel. Gupta and Gupta [28] have studied the radiation effect on a hydro magnetic convective flow in a vertical channel. Datta and Jana [18] have studied the effect of wall conductance on a hydro magnetic convection of a radiation gas in a vertical channel. The combined forced and free convective flow in a vertical channel with viscous dissipation and isothermal – iso flux boundary conditions have been studied by Barletta [9]. Barletta *et al.* [10] have presented a dual mixed convection flow in a vertical channel. Barletta *et al.* [11] have described a buoyancy MHD flow in a vertical channel.

Non – Darcy effects on natural convection in porous media have received a great deal of attention in recent years because of the experiments conducted with several combinations of solids and fluids covering wide ranges of governing parameters which indicate that the experimental data for systems other than glass water at low Rayleigh numbers, do not agree with theoretical predictions based on the Darcy flow model. This divergence in the heat transfer results has been reviewed in detail in Cheng [16] and Prasad *et al.* [44] among others. Extensive effects are thus being made to include the inertia and viscous diffusion terms in the flow equations and to examine their effects in order to develop a reasonable accurate mathematical model for convective transport in porous media. The work of Vafai and Tien [62] was one of the early attempts to account for the boundary and inertia effects in the momentum equation for a porous medium. They found that the momentum boundary layer thickness is of order of $\sqrt{\frac{k}{\varepsilon}}$. Vafai and Thiyagaraja [63] presented analytical solutions for the velocity and temperature fields for the interface region using the Brinkman

Corresponding Author: B. Haritha, [2]Department of Mathematics,*
Sri Krishnadevaraya University, Ananthapuramu -515003, (A.P.), India.

Forchheimer –extended Darcy equation. Detailed accounts of the recent efforts on non-Darcy convection have been recently reported in Tien and Hong [59], Cheng [16] and Kalidas and Prasad [31]. Here, we will restrict our discussion to the vertical cavity only. Poulikakos and Bejan [45] investigated the inertia effects through the inclusion of Forchheimer velocity squared term, and presented the boundary layer analysis for tall cavities. They also obtained numerical results for a few cases in order to verify the accuracy of their boundary layer analysis for tall cavities. They also obtained numerical results for a few cases in order to verify the accuracy of their boundary layer solutions. Later, Prasad and Tuntomo [43] reported an extensive numerical work for a wide range of parameters, and demonstrated that effects of Prandatl number remain almost unaltered while the dependence on the modified Grashof number, G, changes significantly with an increase in the Forchheimer number. This result in reversal of flow regimes from boundary layer to asymptotic to conduction as the contribution of the inertia term increases in comparison with that of the boundary term. They also reported a criterion for the Darcy flow limit. The Brinkman – Extended – Darcy modal was considered in Tong and Subramanian [60], and Lauriat and Prasad [34] to examine the boundary effects on free convection in a vertical cavity. While Tong and Subramanian performed a Weber – type boundary layer analysis, Lauriat and Prasad solved the problem numerically for A=1 and5. It was shown that for a fixed modified Rayleigh number, Ra, the Nusselt number; decrease with an increase in the Darcy number; the reduction being larger at higher values of Ra. A scale analysis as well as the computational data also showed that the transport term $(v.\nabla)v$, is of low order of magnitude compared to the diffusion plus buoyancy terms. A numerical study based on the Forchheimer-Brinkman-Extended Darcy equation of motion has also been reported recently by Beckerman *et al.* [12]. They demonstrated that the inclusion of both the inertia and boundary effects is important for convection in a rectangular packed – sphere cavity. Umadevi *et al.* [61] have studied the chemical reaction effect on Non-Darcy convective heat and mass transfer flow through a porous medium in a vertical channel with heat sources. Deepthi *et al.* [19] and Kamalakar *et al.* [32] have discussed the numerical study of non-Darcy convective heat and mass transfer flow in a vertical channel with constant heat sources under different conditions.

The effect of radiation on MHD flow and heat transfer problem has become more important industrially. At high operation temperature, radiation effect can be quite significant. Many processes in engineering areas occur at high temperature and knowledge of radiation heat transfer becomes very important for the design of the pertinent equipment. Nuclear power plants, gas turbines and the various propulsion devices for aircraft, missiles, satellites and space vehicles are examples of such engineering areas. Abdul Sattar [1] investigated the unsteady free convection interaction with thermal radiation in a boundary layer flow past a vertical porous plate. Mankinde [37] examined the transient free convection interaction with thermal radiation of an absorbing-emitting fluid along moving vertical permeable plate Raptis [48] analyzed the thermal radiation and free convection flow through a porous medium by using perturbation technique. Bakier and Gorla [7] investigated the effect of thermal radiation on mixed convection from horizontal surfaces in saturated porous media. Chamkha [15] studied the solar radiation effects on porous media supported by a vertical plate. Forest fire spread also constitutes an important application of radiative convective heat transfer. The thermal radiation effects on heat transfer in magneto – aerodynamic boundary layers has also received some attention, owing to astronautical re-entry, plasma flows in astrophysics, the planetary magneto-boundary layer and MHD propulsion systems. Mosa [38] discussed one of the first models for combined radiative hydromagnetic heat transfer, considered the case of free convective channel flows with an axial temperature gradient. Nath *et al.* [40] obtained a set of similarity solutions for radiative – MHD stellar point explosion dynamics using shooting methods. Shateyi *et al.* [54] have analyzed the Thermal Radiation and Buoyancy Effects on Heat and Mass Transfer over a Semi-Infinite stretching Surface with Suction and Blowing. Dulal Pal et al [20] have discussed Heat and Mass transfer in MHD non-Darcian flow of a micropolar fluid over a stretching sheet embedded in a porous media with non-uniform heat source and thermal radiation. Dulal Pal *et al.* [21] have analyzed unsteady magneto hydrodynamic convective heat and mass transfer in a boundary layer slip flow past a vertical permeable plate with thermal radiation and chemical reaction. Rajesh *et al.* [47] have considered the radiation effects on MHD flow through a porous medium with variable temperature or variable mass diffusion. .

When heat and mass transfer occur simultaneously in a moving fluid, the relation between the fluxes and the driving potentials are of more intricate nature. Mass fluxes can be created by temperature gradients and this is the Soret effect or thermo-diffusion effect. Adrian Postelnicu [2] has studied thermo-diffusion and diffusion thermo effects on combined heat and mass transfer through a porous medium under different conditions. All the above mentioned studies are based on the hypothesis that the effect of dissipation is neglected. This is possible in case of ordinary fluid flow like air and water under gravitational force. But this effect is expected to be relevant for fluids with high values of the dynamic viscosity force. In view of this, several authors, notably Soundalgekar and Pop [56], Barletta [8], Zanchini [65] and Sreevani [55] have studied the effect of viscous dissipation on the convective flows past an infinite vertical plate and through vertical channels and ducts. Indudhar *et al.* [30] have investigated the effect of thermo-diffusion on convective heat and mass transfer in a vertical channel. Madhusudhan Reddy *et al.* [36] have investigated the effect of thermo-diffusion and chemical reaction on non-darcy convective heat and mass transfer flow in a vertical channel with radiation. Kamalakar *et al.* [32] have discussed the finite element analysis of chemical reaction effect on non-darcy convective heat and mass transfer flow through a porous medium in a vertical channel with heat sources. Rajasekhar *et. al.* [46] have analyzed the effect of Hall current, thermal radiation and thermo-diffusion on convective heat and mass

transfer flow of a viscous rotating fluid past a vertical porous plate embedded in a porous medium. Muthucumaraswamy *et al.* [39] have studied the rotation effects on flow past an accelerated isothermal vertical plate with chemical reaction of first order. Jafarunnisa [29] has discussed the effect of thermal radiation and thermo diffusion on unsteady convective heat and mass transfer flow in the rotating system with heat sources. Alam *et al.* [6] have discussed the steady MHD combined heat and mass transfer flow through a porous medium past an infinite vertical plate with viscous dissipation and joule heating effects in a rotating system. Kafoussias and Williams *et.al.* [33] studied the effects of thermal-diffusion and diffusion thermo on steady mixed free-forced convective and mass transfer over a vertical flat plate, when the viscosity of the fluid varies with temperature. Alam *et al.* [3] studied the effects of Dufour and Soret numbers on unsteady free convection and mass transfer flow past an impulsively started infinite vertical porous flat plate, of a viscous incompressible and electrically conducting fluid, in the presence of an uniform transverse magnetic field. Alam *et al.* [4] studied the effects of Dufour and Soret numbers on unsteady MHD free convection and mass transfer flow past an infinite vertical porous plate embedded in a porous medium. Lakshminarayana *et al.* [35] have investigated Soret and Dufour effects on free convection along vertical wavy surface in a fluid saturated darcy porous medium. Naga Radhika, *et al.* [41] Dissipative and radiation effects on heat transfer flow of a viscous fluid in a vertical channel. Dulal pal *et al.* [22] have studied the effect of Soret, Dufour, chemical reaction and thermal radiation on MHD, non-darcy, unsteady mixed convective heat and mass transfer over stretching sheet. Ching-Yang-Cheng [17] have investigated Soret and Dufour effects on free convective boundary layer over inclined wavy surface in a porous medium. Dulal pal, *et al.* [23] have investigated the effects on MHD non-darcian mixed convective heat and mass transfer over a stretching sheet with non-uniform heat source/sink. Sulochana and Tayappa, *et al.* [57] Finite element analysis of thermo-diffusion and diffusion- thermo effects on combined heat and mass transfer flow of viscous, electrically conducting fluid through a porous medium in vertical channel. Ramana Reddy, *et al.* [53] Thermal diffusion and chemical reaction effects on unsteady MHD dusty viscous flow. Raju, *et al.* [50] Radiation, Inclined Magnetic field and Cross-Diffusion effects on flow over a stretching surface. Raju, *et al.* [51] Radiation and chemical reaction effects on thermo-phoretic MHD flow over an aligned isothermal permeable surface with heat source. Raju, *et al.* [52] Radiation and soret effects of MHD nanofluid flow over a moving vertical plate in porous medium.

All the above mentioned studies are based on the hypothesis that the effect of dissipation is neglected. This is possible in case of ordinary fluid flow like air and water under gravitational force. But this effect is expected to be relevant for fluids with high values of the dynamic viscosity force. Moreover Gebhart and Mollendorf [25] have shown that viscous dissipation heat in the natural convective flow is important when the fluid is of extreme size or is at extremely low temperature or in high gravitational field.

Keeping the above application in view we made an attempt has been made to investigate the effect of dissipation and thermal radiation on convective heat and mass transfer in a vertical channel. The Brinkman Forchheimer extended Darcy equations which take into account the boundary and inertia effects are used in the governing linear Momentum equation. In order to obtain a better insight into this complex problem, we make use of Galerkin finite element analysis with Quadratic Polynomial approximations. The velocity, temperature, concentration, shear stress and rate of Heat and Mass transfer are evaluated numerically for different variations of parameter.

In this paper we investigate the effect of dissipation and thermal radiation on convective heat and mass transfer in a vertical channel with Soret and Dufour effects using Galerkin finite element technique. The governing equations of flow heat and mass transfer have been solved to obtain Velocity, Temperature and Concentration. The effects of dissipation and thermal radiation on the flow characteristics have been investigated.

2. FORMULATION OF THE PROBLEM

We consider a fully developed laminar convective heat and mass transfer flow of a viscous fluid through a porous medium confined in a vertical channel bounded by flat walls. We choose a Cartesian co-ordinate system O(x, y, z) with x- axis in the vertical direction and y-axis normal to the walls. The walls are taken at y=±L. The walls are maintained at constant temperature and concentration. The temperature gradient in the flow field is sufficient to cause natural convection in the flow field. A constant axial pressure gradient is also imposed so that this resultant flow is a mixed convection flow. The porous medium is assumed to be isotropic and homogeneous with constant porosity and effective thermal diffusivity. The thermo physical properties of porous matrix are also assumed to be constant and Boussinesq approximation is invoked by confining the density variation to the buoyancy term. In the absence of any extraneous force flow is unidirectional along the x-axis which is assumed to be infinite.

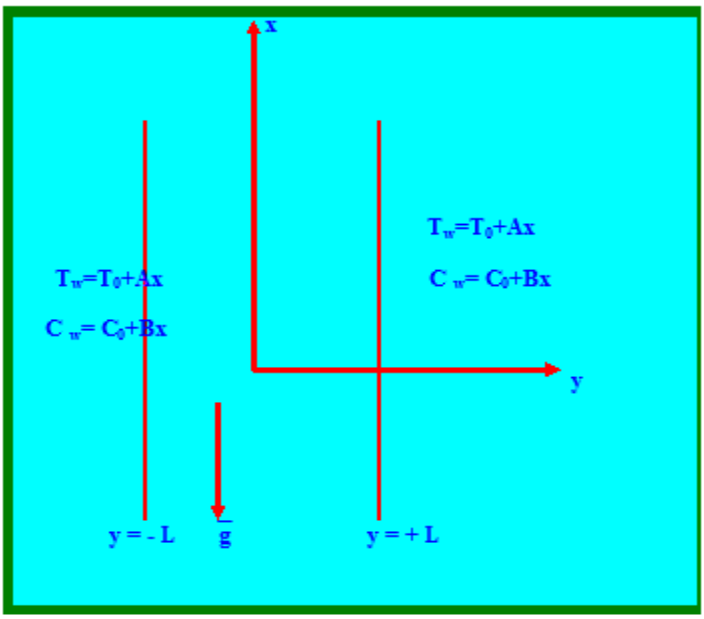

Figure-1: Configuration of the problem

The momentum, energy and diffusion equations in the scalar form are

$$-\frac{\partial p}{\partial x}+\left(\frac{\mu}{\delta}\right)\frac{\partial^2 u}{\partial y^2}-\left(\frac{\mu}{k}\right)u-\left(\frac{\sigma\mu_e^2 H_o^2}{\rho_e}\right)u-\frac{\rho\delta F}{\sqrt{k}}u^2-\rho g=0 \tag{1}$$

$$\rho_0 C_p u\frac{\partial T}{\partial x}=k_f\frac{\partial^2 T}{\partial y^2}-\frac{\partial(q_R)}{\partial y}+\mu\left(\frac{\partial u}{\partial y}\right)^2+\frac{DmK_T}{C_s C_p}\frac{\partial^2 C}{\partial y^2} \tag{2}$$

$$u\frac{\partial C}{\partial x}=D_1\frac{\partial^2 C}{\partial y^2}-k_1 C+\frac{D_m K_T}{T_m}\frac{\partial^2\theta}{\partial y^2} \tag{3}$$

The relevant boundary conditions are

$$u=0,\quad T=T_w,\quad C=C_w \text{ at } \quad y=\pm L \tag{4}$$

where u, T, C are the velocity, temperature and Concentration, p is the pressure ,ρ is the density of the fluid, Cp is the specific heat at constant pressure, μ is the coefficient of viscosity, k is the permeability of the porous medium, δ is the porosity of the medium,β is the coefficient of thermal expansion, k_f is the coefficient of thermal conductivity, F is a function that depends on the Reynolds number and the microstructure of porous medium, $\beta^{\bullet}$ is the volumetric coefficient of expansion with mass fraction concentration, k_1 is the chemical reaction coefficient and D_1 is the chemical molecular diffusivity, q_R is the radiative heat flux, Dm is the coefficient of mass diffusivity, K_T thermo-diffusion ratio, Tm is the mean fluid temperature Here, the thermo physical properties of the solid and fluid have been assumed to be constant except for the density variation in the body force term (Boussinesq approximation) and the solid particles and the fluids are considered to be in the thermal equilibrium.

By applying Rosseland approximation (Brewester [7a]) the radiative heat flux q_r is given by

$$q_r=-\left(\frac{4\sigma^*}{3\beta_R}\right)\frac{\partial}{\partial y}\left[T'^4\right] \tag{5}$$

Where σ* is the Stephan – Boltzmann constant and mean absorption coefficient.

Assuming that the difference in temperature within the flow, such that T'^4 can be expressed as a linear combination of the temperature. We expand T'^4 in Taylor's series about Te as follows

$$T'^4=T_\infty^4+4T_\infty^3(T-T_\infty)+6T_\infty^2(T-T_\infty)+\ldots\ldots \tag{6}$$

Neglecting higher order terms beyond the first degree in $(T-T_\infty)$ .we have

$$T'^4\simeq -3T_\infty^4+4T_\infty^3 T \tag{7}$$

Differentiating equation (5) with respect to y and using (7) we get

$$\frac{\partial(q_R)}{\partial y} = -\frac{16\sigma^* T_\infty^3}{3\beta_R}\frac{\partial^2 T}{\partial y^2} \tag{8}$$

Using (8) equation (2) reduces to

$$\rho_0 C_p u\frac{\partial T}{\partial x} = \left(k_f + \frac{16\sigma^* T_e^3}{3\beta_R}\right)\frac{\partial^2 T}{\partial y^2} + \mu\left(\frac{\partial u}{\partial y}\right)^2 + \frac{DmK_T}{C_s C_p}\frac{\partial^2 C}{\partial y^2} \tag{9}$$

Following Tao [43], we assume that the temperature and concentration of the both walls is $T_w = T_0 + Ax$, $C_w = C_0 + Bx$ where A and B are the vertical temperature and concentration gradients which are positive for buoyancy –aided flow and negative for buoyancy –opposed flow, respectively, T_0 and C_0 are the upstream reference wall temperature and concentration respectively. The velocity depend only on the radial coordinate and all the other physical variables except temperature, concentration and pressure are functions of y and x, x being the vertical co-ordinate.

The temperature and concentration inside the fluid can be written as

$$T = T^\bullet(y) + Ax, \qquad C = C^\bullet(y) + Bx$$

We define the following non-dimensional variables as

$$\begin{aligned} &u' = \frac{u}{(\nu / L)},\ (x', y') = (x, y)/L,\quad p' = \frac{p\delta}{(\rho\nu^2 / L^2)} \\ &\theta(\mathrm{y}) = \frac{\mathrm{T^\bullet\text{-}T_0}}{\mathrm{P_1 AL}},\quad \mathrm{C} = \frac{\mathrm{C^\bullet\text{-}C_0}}{\mathrm{P_1 BL}}, \mathrm{P_1} = \frac{dp}{dx} \end{aligned} \tag{10}$$

Introducing these non-dimensional variables the governing equations in the dimensionless form reduce to (on dropping the dashes)

$$\frac{d^2u}{dy^2} = 1 + \delta(D^{-1})u - \delta G(\theta + NC) - \delta^2\Delta u^2 \tag{11}$$

$$\left(1 + \frac{4Rd}{3}\right)\frac{d^2\theta}{dy^2} = (P_r)u + Ec\,\mathrm{Pr}\left(\frac{du}{dy}\right)^2 - Du\,\mathrm{Pr}\frac{d^2C}{dy^2} \tag{12}$$

$$\frac{d^2C}{dy^2} - \gamma C = (Sc)u - ScSr\frac{d^2\theta}{dy^2} \tag{13}$$

Where

$\Delta = FD^{-1/2}$ (Inertia or Fochhemeir parameter) $\qquad G = \dfrac{\beta g A L^3}{\nu^2}$ (Grashof Number)

$D^{-1} = \dfrac{L^2}{k}$ (Inverse Darcy parameter) $\qquad Sc = \dfrac{\nu}{D_1}$ (Schmidt number)

$N = \dfrac{\beta^\bullet B}{\beta A}$ (Buoyancy ratio) $\qquad P_r = \dfrac{\mu C_p}{k_f}$ (Prandtl Number)

$\gamma = \dfrac{k_1 L^2}{D_1}$ (Chemical reaction parameter) $\qquad Rd = \dfrac{4\sigma^* T_e^3}{3\beta_r k_f}$ (Radiation Parameter)

$Ec = \dfrac{\nu^2}{P_1 A L^3 C_p}$ (Eckert number)` $\qquad Sr = \dfrac{D_m K_T A}{k_f T_m B}$ (Soret Parameter)

$Du = \dfrac{D_m K_T B}{C_S C_p A}$ (Dufour Parameter)

The corresponding boundary conditions are

$$u = 0,\ \ \theta = 0,\ C = 0 \quad on\ y = \pm 1 \tag{14}$$

3. FINITE ELEMENT ANALYSIS

To solve these differential equations with the corresponding boundary conditions, we assume if u^i, θ^I, c^i are the approximations of u, θ and C we define the errors (residual) E_u^i, E_θ^i, E_c^i as

$$E_u^i = \frac{d}{d\eta}\left(\frac{du^i}{d\eta}\right) - D^{-1}u^i + \delta^2 \mathrm{A}(u^i)^2 - \delta G(\theta^i + NC^i) \tag{15}$$

$$E_c^i = \frac{d}{dy}\left(\frac{d}{dy}{}^i C\right) - \gamma C^i - Scu^i - ScSr\frac{d}{dy}\left(\frac{d\theta^i}{dy}\right) \tag{16}$$

$$E_\theta^i = \left(1 + \frac{4Rd}{3}\right)\frac{d}{dy}\left(\frac{d\theta^i}{dy}\right) - P_r u^i - P_r Ec\left(\frac{d}{dy}{}^i u\right)^2 - Du\,\mathrm{Pr}\frac{d}{dy}\left(\frac{d}{dy}{}^i C\right) \tag{17}$$

Where

$$u^i = \sum_{k=1}^{3} u_k \psi_k \qquad C^i = \sum_{k=1}^{3} C_k \psi_k \qquad \theta^i = \sum_{k=1}^{3} \theta_k \psi_k \tag{18}$$

These errors are orthogonal to the weight function over the domain of e^i under Galerkin finite element technique we choose the approximation functions as the weight function. Multiply both sides of the equations (11-13) by the weight function i.e. each of the approximation function ψ_j^i and integrate over the typical three nodded linear element (η_e, η_{e+1}) we obtain

Where

$$\int_{\eta_e}^{\eta_{e+1}} \left(\frac{d}{d\eta}\left(\frac{du^i}{d\eta}\right) - D^{-1}u^i + \delta^2 \mathrm{A}(u^i)^2 - \delta G(\theta^i + NC^i\right)\psi_j^i dy = 0 \tag{19}$$

$$\int_{\eta_e}^{\eta_{e+1}} \left(\frac{d}{dy}\left(\frac{d}{dy}{}^i C\right) - \gamma C^i - Scu^i + ScSr\frac{d}{dy}\left(\frac{d\theta^i}{dy}\right)\right)\psi_j^i dy = 0 \tag{20}$$

$$\int_{\eta_e}^{\eta_{e+1}} \left(1 + \frac{4Rd}{3}\right)\frac{d}{dy}\left(\frac{d\theta^i}{dy}\right) - P_r u^i - P_r Ec\left(\frac{d\theta^i}{dy}\right)^2 + Du\,\mathrm{Pr}\frac{d}{dy}\left(\frac{d}{dy}{}^i C\right)\psi_j^i dy = 0 \tag{21}$$

Choosing different Ψ_j^i's corresponding to each element η_e in the equation (19)-(21) yields a local stiffness matrix of order 3×3 in the form

$$(f_{i,j}^k)(u_i^k) - \delta G(g_{i.j}^k)(\theta_i^k + NC_i^k) + \delta D^{-1}(m_{i.j}^k)(u_i^k) + \delta^2 \mathrm{A}(n_{i.j}^k)(u_i^k) = (Q_{i,j}^k) + (Q_{2,j}^k) \tag{22}$$

$$((e_{i,J}^k) - \gamma)(C_i^k) - Sc(m_{i.j}^k)(u_i^k) + ScS\,\mathrm{r}(r_{i,j}^k)(\theta_i^k) = R_{1J}^k + R_{2J}^k \tag{23}$$

$$\left(1 + \frac{4Rd}{3}\right)(l_{iJ}^k))(\theta_i^k) - (P_r(1+E_c))(t_{iJ}^k)(u_i^k) + Du\,\mathrm{Pr}(p_{i,j}^k)(C_i^k) = S_{1,J}^k + S_{2,J}^k \tag{24}$$

Where

$(f_{i,J}^k)$, $(g_{i,J}^k)$, $(m_{i,J}^k)$, $(n_{i,J}^k)$, $(e_{i,J}^k)$, (t_{iJ}^k), $(p_{i,J}^k)$, (r_{iJ}^k) are 3×3 matrices and $(Q_{2,J}^k)$, $(Q_{1,J}^k)$, $(R_{2,J}^k)$, (R_{1J}^k), (S_{2J}^k) and (S_{1J}^k) are 3×1 column matrices and such stiffness matrices in terms of local nodes in each element are assembled using inter element continuity and equilibrium conditions to obtain the coupled global matrices in terms of the global nodal values of u, θ & C((22)-(24)). The resulting coupled stiffness matrices are solved by iteration process. This procedure is repeated till the consecutive values of u_i's, θ_i's and C_i's differ by a pre assigned percentage.

The shape functions corresponding to

$$\Psi_1^1=\frac{(y-4)(y-8)}{32} \qquad \Psi_2^1=\frac{(y-12)(y-16)}{32} \qquad \Psi_3^1=\frac{(y-20)(y-24)}{32}$$

$$\Psi_1^2=\frac{(y-2)(y-4)}{8} \qquad \Psi_2^2=\frac{(y-6)(y-8)}{8} \qquad \Psi_2^3=\frac{(y-10)(y-12)}{8}$$

$$\Psi_1^3=\frac{(3y-4)(3y-8)}{32} \qquad \Psi_2^3=\frac{(3y-12)(3y-16)}{32} \qquad \Psi_3^3=\frac{(3y-20)(3y-24)}{32}$$

$$\Psi_1^4=\frac{(y-1)(y-2)}{2} \qquad \Psi_2^4=\frac{(y-3)(y-4)}{2} \qquad \Psi_3^4=\frac{(y-5)(y-6)}{2}$$

$$\Psi_1^5=\frac{(5y-4)(5y-8)}{32} \qquad \Psi_2^5=\frac{(5y-12)(5y-16)}{32} \qquad \Psi_3^5=\frac{(5y-20)(5y-24)}{32}$$

4. STIFFNESS MATRICES

The global matrix for θ is

$$A_3\,X_3 = B_3 \tag{5.25}$$

The global matrix for C is

$$A_4\,X_4 = B_4 \tag{5.26}$$

The global matrix u is

$$A_5\,X_5 = B_5 \tag{5.27}$$

Where

$$B_3=\begin{bmatrix}
-1 & a_{12} & a_{13} & 0 & 0 & 0 & 0 & 0 & 0 & 0 & 0\\
0 & a_{22} & a_{23} & 0 & 0 & 0 & 0 & 0 & 0 & 0 & 0\\
0 & a_{32} & a_{33} & 0 & a_{35} & 0 & 0 & 0 & 0 & 0 & 0\\
0 & 0 & a_{44} & a_{44} & a_{45} & 0 & 0 & 0 & 0 & 0 & 0\\
0 & 0 & a_{53} & a_{54} & a_{55} & a_{56} & a_{57} & 0 & 0 & 0 & 0\\
0 & 0 & 0 & a_{64} & a_{65} & a_{66} & a_{67} & 0 & 0 & 0 & 0\\
0 & 0 & 0 & 0 & a_{75} & a_{76} & a_{77} & a_{78} & a_{79} & 0 & 0\\
0 & 0 & 0 & 0 & 0 & 0 & a_{87} & a_{88} & a_{89} & 0 & 0\\
0 & 0 & 0 & 0 & 0 & 0 & a_{97} & a_{98} & a_{99} & a_{910} & 0\\
0 & 0 & 0 & 0 & 0 & 0 & 0 & 0 & a_{109} & a_{1010} & 0\\
0 & 0 & 0 & 0 & 0 & 0 & 0 & 0 & a_{119} & a_{1110} & -1
\end{bmatrix}$$

$$B_4=\begin{bmatrix}
1 & b_{1,2} & b_{1,3} & 0 & 0 & 0 & 0 & 0 & 0 & 0 & 0\\
0 & b_{2,2} & b_{2,3} & 0 & 0 & 0 & 0 & 0 & 0 & 0 & 0\\
0 & b_{3,2} & b_{3,3} & 0 & b_{3,5} & 0 & 0 & 0 & 0 & 0 & 0\\
0 & 0 & b_{4,4} & b_{4,4} & b_{4,5} & 0 & 0 & 0 & 0 & 0 & 0\\
0 & 0 & b_{5,3} & b_{5,4} & b_{5,5} & b_{5,6} & b_{5,7} & 0 & 0 & 0 & 0\\
0 & 0 & 0 & b_{6,4} & b_{6,5} & b_{6,6} & b_{6,7} & 0 & 0 & 0 & 0\\
0 & 0 & 0 & 0 & b_{7,5} & b_{7,6} & b_{7,7} & b_{7,8} & b_{7,9} & 0 & 0\\
0 & 0 & 0 & 0 & 0 & 0 & b_{8,7} & b_{8,8} & b_{8,9} & 0 & 0\\
0 & 0 & 0 & 0 & 0 & 0 & b_{9,7} & b_{9,8} & b_{9,9} & b_{9,10} & 0\\
0 & 0 & 0 & 0 & 0 & 0 & 0 & 0 & b_{10,9} & b_{11,10} & 0\\
0 & 0 & 0 & 0 & 0 & 0 & 0 & 0 & b_{11,9} & b_{11,10} & b_{11,11}
\end{bmatrix}$$

$$B_5 = \begin{bmatrix} 1 & a_{1,2} & a_{1,3} & 0 & 0 & 0 & 0 & 0 & 0 & 0 & 0 \\ 0 & a_{2,2} & a_{2,3} & 0 & 0 & 0 & 0 & 0 & 0 & 0 & 0 \\ 0 & a_{3,2} & a_{3,3} & 0 & a_{3,5} & 0 & 0 & 0 & 0 & 0 & 0 \\ 0 & 0 & a_{4,4} & a_{4,4} & a_{4,5} & 0 & 0 & 0 & 0 & 0 & 0 \\ 0 & 0 & a_{5,3} & a_{5,4} & a_{5,5} & a_{5,6} & a_{5,7} & 0 & 0 & 0 & 0 \\ 0 & 0 & 0 & a_{6,4} & a_{6,5} & a_{6,6} & a_{6,7} & 0 & 0 & 0 & 0 \\ 0 & 0 & 0 & 0 & a_{7,5} & a_{7,6} & a_{7,7} & a_{7,8} & a_{7,9} & 0 & 0 \\ 0 & 0 & 0 & 0 & 0 & 0 & a_{8,7} & a_{8,8} & a_{8,9} & 0 & 0 \\ 0 & 0 & 0 & 0 & 0 & 0 & a_{9,7} & a_{9,8} & a_{9,9} & a_{9,10} & 0 \\ 0 & 0 & 0 & 0 & 0 & 0 & 0 & 0 & b_{10,9} & b_{11,10} & 0 \\ 0 & 0 & 0 & 0 & 0 & 0 & 0 & 0 & b_{11,9} & b_{11,10} & b_{11,11} \end{bmatrix}$$

$$X_3 = \begin{bmatrix} \theta_1 \\ \theta_2 \\ \theta_3 \\ \theta_4 \\ \theta_5 \\ \theta_6 \\ \theta_7 \\ \theta_8 \\ \theta_9 \\ \theta_{10} \\ \theta_{11} \end{bmatrix}, X_4 = \begin{bmatrix} C_1 \\ C_2 \\ C_3 \\ C_4 \\ C_5 \\ C_6 \\ C_7 \\ C_8 \\ C_9 \\ C_{10} \\ C_{11} \end{bmatrix}, X_5 = \begin{bmatrix} \psi_1 \\ \psi_2 \\ \psi_3 \\ \psi_4 \\ \psi_5 \\ \psi_6 \\ \psi_7 \\ \psi_8 \\ \psi_9 \\ \psi_{10} \\ \psi_{11} \end{bmatrix}, B_3 = \begin{bmatrix} \frac{ar}{1} \\ \frac{ar}{2} \\ \frac{ar}{3} \\ \frac{ar}{4} \\ \frac{ar}{5} \\ \frac{ar}{6} \\ \frac{ar}{7} \\ \frac{ar}{8} \\ \frac{ar}{9} \\ \frac{ar}{10} \\ \frac{ar}{11} \end{bmatrix}, B_4 = \begin{bmatrix} \frac{hr}{1} \\ \frac{hr}{2} \\ \frac{hr}{3} \\ \frac{hr}{4} \\ \frac{hr}{5} \\ \frac{hr}{6} \\ \frac{hr}{7} \\ \frac{hr}{8} \\ \frac{hr}{9} \\ \frac{hr}{10} \\ \frac{hr}{11} \end{bmatrix}, B_5 = \begin{bmatrix} \frac{f}{1} \\ \frac{f}{2} \\ \frac{f}{3} \\ \frac{f}{4} \\ \frac{f}{5} \\ \frac{f}{6} \\ \frac{f}{7} \\ \frac{f}{8} \\ \frac{f}{9} \\ \frac{f}{10} \\ \frac{f}{11} \end{bmatrix}$$

In fact the non-linear term arises in the modified Brinkman linear momentum equation of the porous medium. The iteration procedure in taking the global matrices is as follows. We split the square term into a product term and keeping one of them say u_i's under integration, the other is expanded in terms of local nodal values, resulting in the corresponding coefficient matrix $(n^k_{i\ j}{}'s)$, whose coefficients involve the unknown u_i's. To evaluate the initial global nodal values of u_i's as zeros in the zeroth approximation. We evaluate u_i's, θ_i's and C_i's in the usual procedure mentioned earlier. Later choosing these values of u_i's as first order approximation calculate θ_i's, C_i's. In the second iteration, we substitute for u_i's the first order approximation of and u_i's and the first approximation of θ_i's and C_i's obtain second order approximation. This procedure is repeated till the consecutive values of u_i's, θ_i's and C_i's differ by a pre assigned percentage. For computational purpose we choose five elements in flow region.

5. SHEAR STRESS, NUSSELT NUMBER AND SHERWOOD NUMBER

The shear stress on the boundaries $y = \pm 1$ is given by

$$\tau_{y=\pm L} = \mu \left(\frac{du}{dy} \right)_{y=\pm L}$$

In the non-dimensional form is

$$\tau_{y=\pm 1} = \left(\frac{du}{dy} \right)_{y=\pm 1}$$

The rate of heat transfer (Nusselt Number) is given by

$$Nu_{y=\pm i} = \left(\frac{d\theta}{dy} \right)_{y=\pm 1}$$

The rate of mass transfer (Sherwood Number) is given by

$$Sh_{y=\pm 1} = \left(\frac{dC}{dy} \right)_{y=\pm 1}$$

6. COMPARISON

In the absence of thermo-diffusion (Sr=0) and Diffusion-thermo (Du=0) the results are in good agreement with that of Ravindra *et al.* (39a).

Parameters		Ravidra et al(2016)			Present Results		
Rd	Ec	τ(+1)	Nu(+1)	Sh(+)	τ(+1)	Nu(+1)	Sh(+)
0.5	0.01	**1.00603**	**0.390218**	**0.287343**	1.00609	0.390219	0.287346
1.5	0.01	**1.00655**	**0.350332**	**0.228738**	1.00659	0.350340	0.228744
5.0	0.01	**1.00695**	**0.345723**	**0.208739**	1.00701	0.345733	0.208745
0.5	0.03	**1.00702**	**0.345597**	**0.240118**	1.00713	0.345601	0.240127
0.5	0.05	**1.00712**	**0.333583**	**0.235383**	1.00716	0.333593	0.235393

7. DISCUSSION OF THE NUMERICAL RESULTS

In order to get physical Insight into the problem we have carried out numerical calculations for non-dimensional velocity, temperature and spices concentration, skin-friction, Nusselt number and Sherwood number by assigning some specific values to the parameters G, M, D^{-1}, Sc, N, Q, γ, E_c, S_r, D_u, P_r and Δ entering into the problem

7.1. Effects of parameters on velocity profiles

Fig.2a shows the variation of the velocity with Grashof number G. It can be seen from the profiles that the axial velocity reduces withy increase in the thermal buoyancy parameter(G).The maximum of u occurs at y=0.0. Fig.3a represents the u with the Magnetic parameter (M).It is found that the magnitude of the axial velocity increases with increase in M.Fig.4a represents u with inverse Darcy parameter(D^{-1}).The axial velocity increases with increase in D^{-1}. This is due to the fact that when the magnetic field is applied normal to the boundaries, ponder motive force acts in the upward direction to decrease the fluid velocity. Also the presence of the porous medium reduces the resistance to the flow resulting in the enhancement of the velocity field. Fig.6a exhibits the variation of u with buoyancy ratio (N). It is found that when the molecular buoyancy force dominates over the thermal buoyancy force the axial velocity decreases when the buoyancy forces are in the same direction and for the forces acting in opposite directions it enhances in the flow region. Fig.5a shows the variation of u with Schmidt number (Sc). It is found that the velocity reduces with increases in Sc. This is due to the fact that increasing Sc means reducing molecular diffusivity. Therefore lesser the molecular diffusivity smaller the velocity in the fluid region. Fig.8a&9a shows the variation of u with heat source parameter (Q). It is found that an increase on the strength of the heat generating source larger the velocity in the entire flow region while it reduces with that of heat absorbing source .The effect of chemical reaction parameter (γ) on u is exhibited in fig.10a&11a. It is found that the axial velocity enhances with increase in γ in the entire flow region in the degenerating chemical reaction case while in the generating chemical reaction case the velocity enhances with $\gamma \leq 1.5$ and reduces with higher $\gamma \geq 2.5$ in the flow region.Fig.12a shows the variation of u with Eckert number Ec. It is found that higher the dissipative effects smaller the axial velocity in the flow region. The variation of u with Soret parameter Sr/Dufour parameter Du is exhibited in fig.13a.It can be seen from the profiles that increasing Soret parameter Sr(or decreasing Dufour parameter Du larger the axial velocity in the flow region.Fig.14a represents the variation of u with

Forchheimer number Δ. It is found that the axial velocity reduces with increasing Δ. Thus the inclusion of inertia effects reduces the axial velocity. Fig.15a represents the variation of u with Prandtl number (Pr). An increase in Pr reduces the velocity in the flow region. This is due to the fact that increasing Pr decreases the thickness of the momentum boundary layer which in turn reduces the velocity in the flow region.

7.2. Effects of parameters on temperature profiles

The non-dimensional temperature (θ) is shown in figs.2b-15b for different parametric representation. We follow the convention that the non-dimensional temperature (θ) is positive/negative according as the actual temperature $(T^{\bullet})$ is

greater/lesser than the reference temperature T_0. Fig.2b exhibits the temperature with G. It is found that the actual temperature reduces with increase in Grashof number with maximum attained at y=0. Fig 3b shows the variation of θ with M. It can be seen from the profiles that the actual temperature increases with M. With reference to D^{-1} we find that the actual temperature reduces with D^{-1}. This is due to the fact that the thickness of the boundary layer decreases owing to the Darcy drag developed by the porous medium (Fig.4b). Fig.6b shows the variation of θ with buoyancy ratio (N). It is observed from the profiles that when the molecular buoyancy force dominates over the thermal buoyancy force the actual temperature reduces irrespective of the directions of the buoyancy forces in the flow region. Fig.5b represents θ with Sc. It is found that lesser the molecular diffusivity smaller the actual temperature in the entire flow region. Fig.8b&9b exhibit the variation of θ with heat source parameter (Q). It is observed from the profiles that an increase in the strength of the heat generating /absorption source leads to a depreciation in the actual temperature in the flow region. Fig.10b&11b represent θ with chemical reaction parameter (γ). From the profiles we find that the actual temperature reduces with increase in γ in the degenerating chemical reaction case while in the generating chemical reaction case, the actual temperature enhances with increase in γ≤1.5 and for higher γ≥2.5,we notice a depreciation in the actual temperature in the flow region. Fig.12b represents θ with Ec. It is found that higher the dissipation larger the actual temperature. The variation of θ with Soret parameter (Sr) and Dufour parameter Du is exhibited in fig.13b.It5 can be seen from the profiles that increasing Sr(or decreasing Du) larger the actual temperature in the flow region.Fig.14b exhibits θ with Forchheimer number (Δ).We find from the figure that the actual temperature increases with increase in Δ. Thus the inclusion of the inertia effects enhances the actual temperature in the flow region. Fig.15b shows the variation of θ with Prandtl number (Pr).As the Prandtl number increases there is a significant enhancement in the thermal boundary layer with a rise in the actual temperature throughout the flow region, since enhancement of Pr amounts to reduction of thermal diffusion.

.

7.3. Effects of parameters on concentration profiles

The non-dimensional concentration (C) is shown in figs. 2c-15c for different parametric variations. We follow the convention that the non-dimensional concentration (C) is positive/negative according as the actual concentration $(C^{\bullet})$ is greater/lesser than the reference concentration (C_o). Fig.2c shows the variation of Concentration with Grashof number G. It can be seen from the profiles that the actual concentration reduces with increasing G.Fig.3c shows the variation of C with Magnetic parameter (M). It is found that an increase in M increases the actual concentration in the flow region. Fig.4c represents C with D^{-1}. We find that lesser the permeability of the porous medium smaller the actual concentration in the entire flow region. Fig.6c shows the variation of C with buoyancy ratio N. We find that when the molecular buoyancy force dominates over the thermal buoyancy force the actual concentration decreases and for the forces acting in opposite directions it e3nhances in the flow region. Fig.5c shows the variation of C with Sc. It can be seen from the profiles that the actual concentration enhances with increase in Sc. Fig.7c&8c shows the variation of C with heat source parameter (Q). An increase in the strength of the heat generating/absorbing source leads to a reduction in the actual concentration. Fig.10c&11c shows the variation of C with Chemical reaction parameter (γ). It can be seen from the profiles that the actual concentration reduces in the degenerating chemical reaction case while in the generating chemical reaction case the actual concentration reduces with γ≤1.5 and fir higher γ≥2.5,we notice an enhancement in the actual concentration in the entire flow region. Fig.12c represents C with Ec. It can be seen from the profiles that higher the dissipation larger the actual concentration in the flow region.Fig.13c shows the variation of C with Sr and Du. We find from the profiles that increasing Soret parameter Sr(or decreasing Du) smaller the actual concentration in the flow region. Fig.14c shows the concentration with Forchheimer number (Δ).We find that the inclusion of inertia effects reduces the actual concentration in the flow region. Fig.15c. exhibits the variation of C with Prandtl number (Pr). As the Prandtl number increases there is a marginal decrease in the actual concentration. This is due to the fact the enhancement of Prandtl number amounts to reduction of thermal diffusion.

7.4. Effects of parameters on Skin friction, Nusselt number and Sherwood number:

The Skin friction, the rate of heat and mass transfer at the boundaries y=±1 is exhibited in table.1.From the tabular values we find that an increase in G or Sc reduces the skin friction on both the wall y= ± 1. Lesser the permeability of

the porous medium smaller the skin friction on the both the walls. With respect to M, we find the skin friction enhances with increasing in M. The skin friction increases on $y=\pm 1$ with increase in the strength of the heat generating while it reduces with strength of the heat absorption source .When the molecular buoyancy force dominates over the thermal buoyancy force the skin friction reduces on the walls when the buoyancy forces are in the same direction and for the forces acting in opposite directions it increases on the walls. With reference to the chemical reaction parameter(γ) we find that the skin friction enhances on both the walls in both the degenerating/generating chemical reaction cases. Higher the radiative heat flux smaller the skin friction on the walls. The variation of τ with Sr and Du shows that increasing Sr(or decreasing Du) reduces τ on both the walls. An increase in Ec enhances the skin friction on the walls Thus higher the dissipative effects larger the skin friction on the walls. The variation of τ with Forchheimer number Δ indicates that the inclusion of the inertia effects leads to a reduction in the skin friction on both the walls. As the Prandtl number increases ($Pr\leq 1.71$) the skin friction enhances while for higher $Pr\geq 3.71$, we notice a reduction in Skin friction.

The rate of heat transfer (Nusselt number) reduces with increase in $G\leq 30$ and enhances with higher $G\geq 50$.An increase in $M\leq 4$ or $D^{-1}\leq 0.4$ reduces the rate of heat transfer while for higher values of M or D-1 we notice a reversed effect on Nu. Lesser the molecular diffusivity($Sc\leq 1.3$) smaller the rate of heat transfer and for further lowering of the mo9lecular diffusivity larger the Nusselt number on the walls. It reduces on the walls with increasing in the buoyancy ratio ($N>0$) when the buoyancy forces are in the same direction and forces acting in opposite directions it enhances on the walls. The magnitude of Nu reduces on $y=\pm 1$, with increase in the strength of the heat generating source while it enhances with heat absorbing source. With respect to the chemical reaction parameter (γ) we find that the magnitude of Nu reduces in the degenerating chemical reaction case and enhances in the generating chemical reaction case on both the walls. Higher the radiative heat flux smaller the rate of heat transfer on both the walls. The Nusselt number reduces with increasing $Ec\leq 0.05$ smaller the Nusselt number and for still higher $Ec\geq 0.07$, Nu enhances on the walls. Increasing Soret parameter Sr (or decreasing Du) reduces the Nusselt number on both the walls. The inclusion of the inertia effects (Δ) leads to a reduction in Nu. Also lesser the thermal diffusivity larger the rate of heat transfer at the walls.

The rate of mass transfer (Sherwood number) reduces with increase $G\leq 20$ and reduces with hig her $G\geq 30$. An increase in $M\leq 4$ or $D^{-1}\leq 0.4$ reduces the rate of mass transfer while for higher values of M or D^{-1} we notice a reversed effect on Sh. Lesser the molecular diffusivity larger the rate of mass transfer. An increase in $Q>0$ decreases Sh on $y=\pm 1$ while a reversed effect is noticed for $Q<0$.With respect to the chemical reaction parameter (γ) we find that the rate of mass transfer reduces on $y=\pm 1$ in degenerating chemical reaction case while in the generating case it increases on the walls. The rate of mass transfer reduces with increase in $N>0$ and enhances with $N<0$ on both the walls. Higher the radiative heat flux larger Sh .With respect to Soret parameter Sr, and Dufour parameter Du we find that increasing Sr(or decreasing Du) enhances the rate of mass transfer on the both the walls. The variation of Sh with Ec shows that the rate of mass transfer increases with increase in Ec. Inclusion of the inertia effects leads to an enhancement in Sh on the walls. With reference to Pr we find that the rate of mass transfer reduces with increase in Pr and for higher $Pr\geq 3.71$,we notice an enhancement in the rate of mass transfer on the walls.

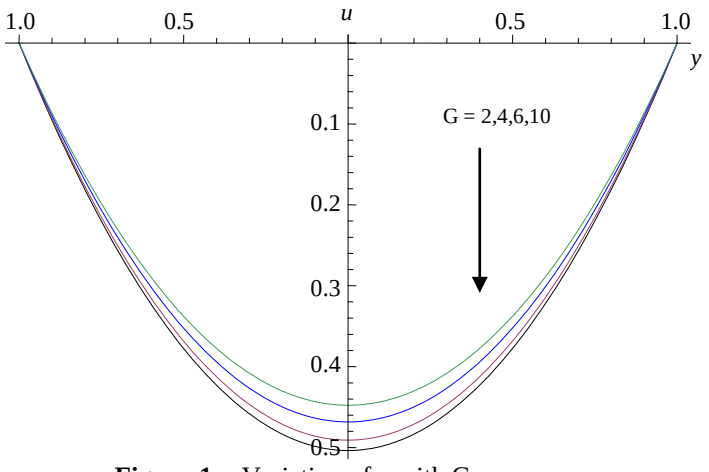

Figure-1a: Variation of u with G
M=2,.D-1=0.2, N=1, Sc=1.3, Ec=0.01, F=0.5, Sr=0.5, Pr=0.71.

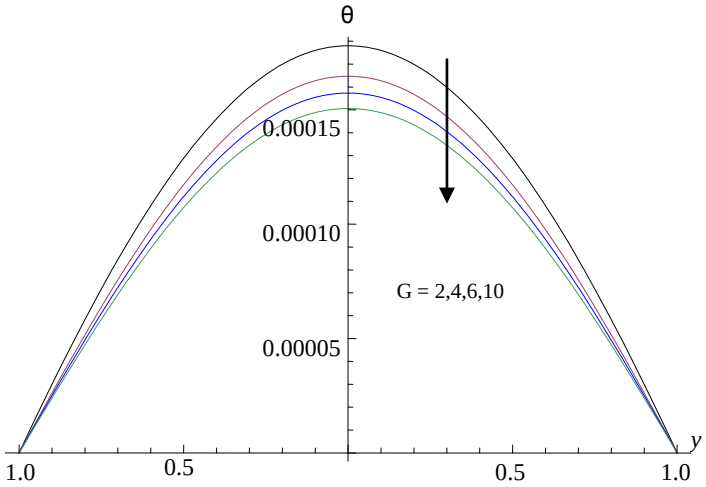

Figure-1b: Variation of temperature with G
M=2, D-1=0.2, N=1, Sc=1.3, Ec=0.01, F=0.5, Sr=0.5, Pr=0.71

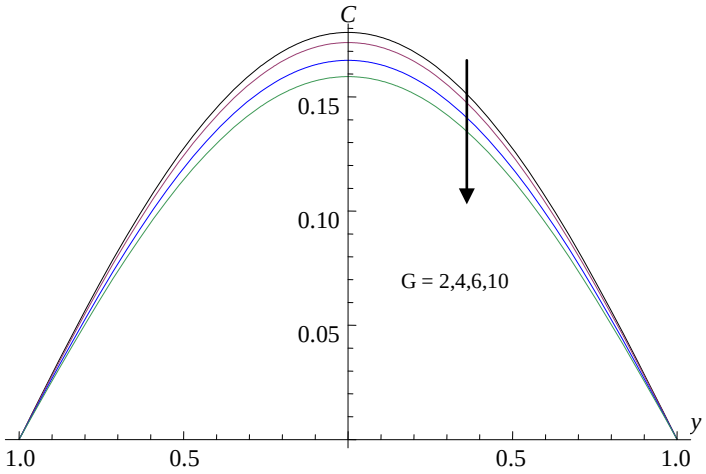

Figure-1c: Variation of Concentration with G
M=2,.D-1=0.2, N=1, Sc=1.3, Ec=0.01, F=0.5, Sr=0.5, Pr=0.71

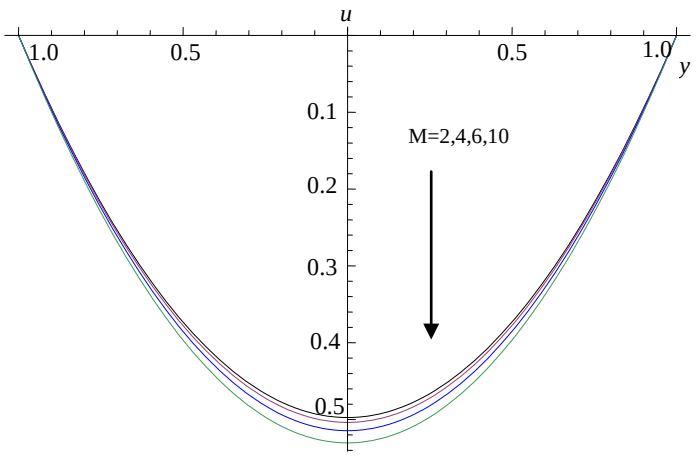

Figure-2a: Variation of u with M
G=2, D-1=0.2, N=1, Sc=1.3, Ec=0.01, F=0.5, Sr=0.5, Pr=0.71.

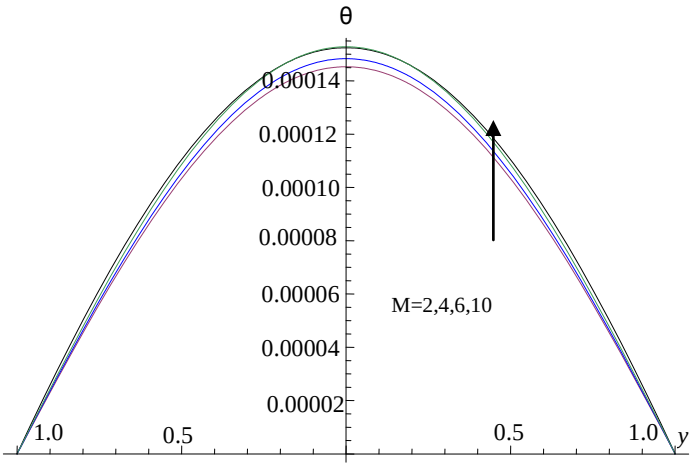

Figure-2b: variation of θ with M
G=2, D-1=0.2, N=1, Sc=1.3, Ec=0.01, F=0.5, Sr=0.5, Pr=0.71.
G=2, D^{-1}=0.2, N=1, Sc=1.3, Ec=0.01, F=0.5, Sr=0.5, Pr=0.71

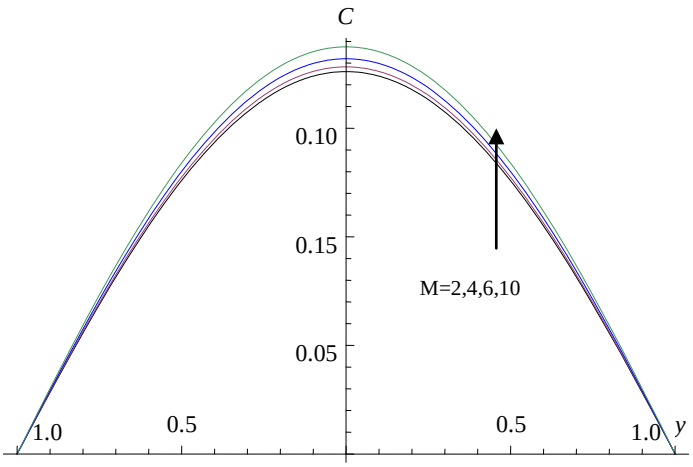

Figure-2c: variation of C with M
G=2,. D-1=0.2, N=1, Sc=1.3, Ec=0.01, F=0.5, Sr=0.5, Pr=0.71.

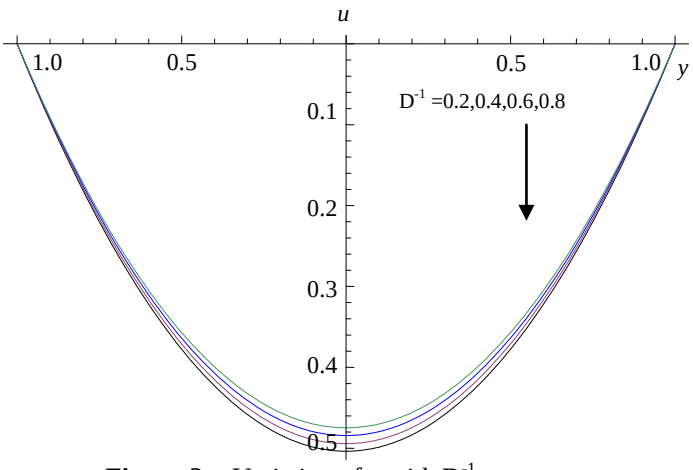

Figure-3a: Variation of u with D^{-1}
G=2, M=2, N=1, Sc=1.3, Ec=0.01, F=0.5, Sr=0.5, Pr=0.71

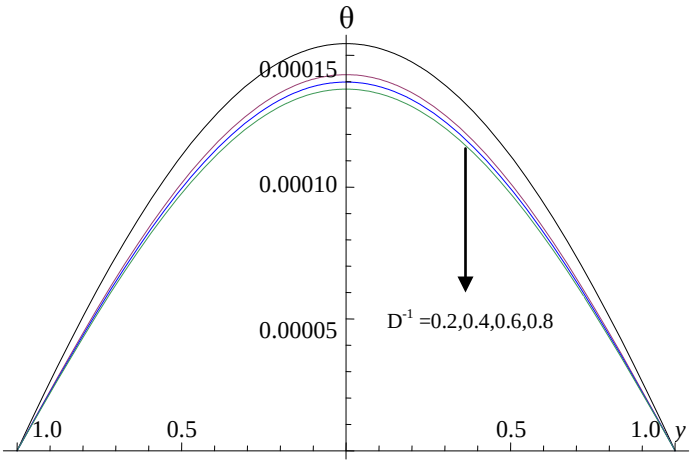

Figure-3b: Variation of θ with D^{-1}
G=2, M=2, N=1, Sc=1.3, Ec=0.01, F=0.5, Sr=0.5, Pr=0.71
G=2, M=2, N=1, Sc=1.3, Ec=0.01, F=0.5, Sr=0.5, Pr=0.71

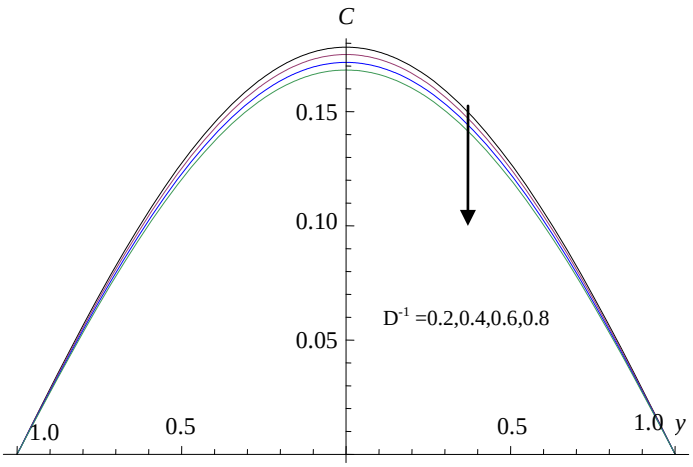

Figure-3c: Variation of C with D^{-1}
G=2, M=2,N=1, Sc=1.3, Ec=0.01, F=0.5, Sr=0.5, Pr=0.71

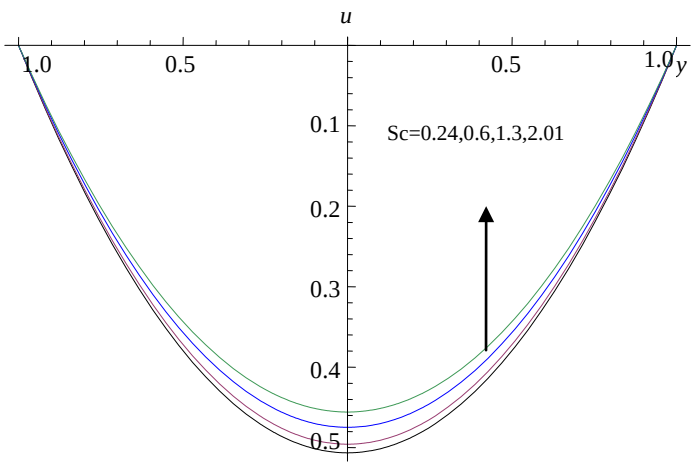

Figure-4a: Variation of u with Sc
G=2, M=2, D^{-1}=0.2, N=1, Ec=0.01, F=0.5, Sr=0.5, Pr=0.71

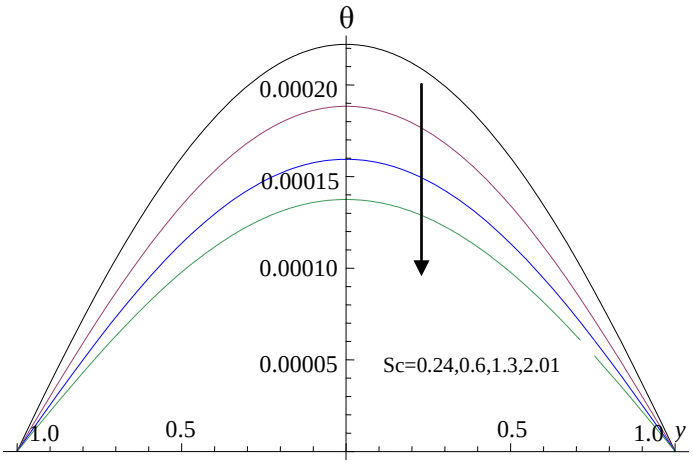

Figure-4b: Variation of θ with Sc
G=2, M=2, D^{-1}=0.2, N=1, Ec=0.01, F=0.5, Sr=0.5, Pr=0.71.

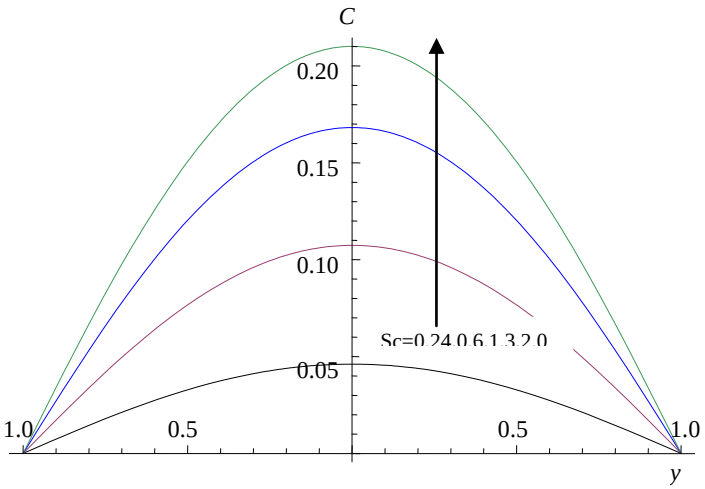

Figure-4c: Variation of C with Sc
G=2, M=2, D^{-1}=0.2, N=1, Ec=0.01, F=0.5, Sr=0.5, Pr=0.71.

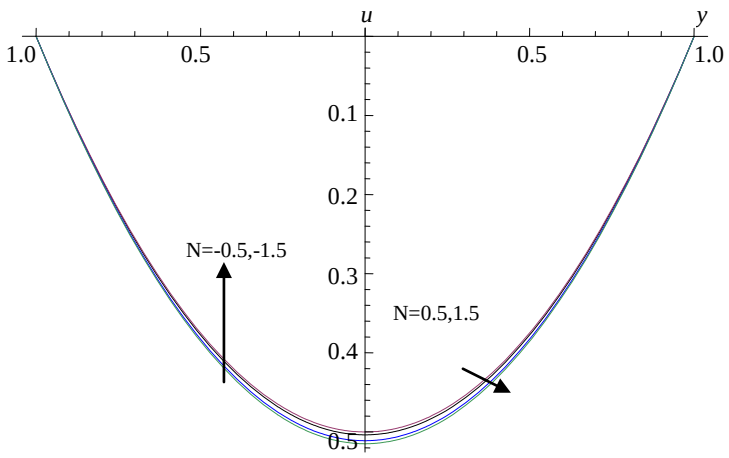

Figure-5a: Variation of u with N
G=2, M=2, D^{-1}=0.2, Sc=1.3, Ec=0.01, F=0.5, Sr=0.5, Pr=0.71.

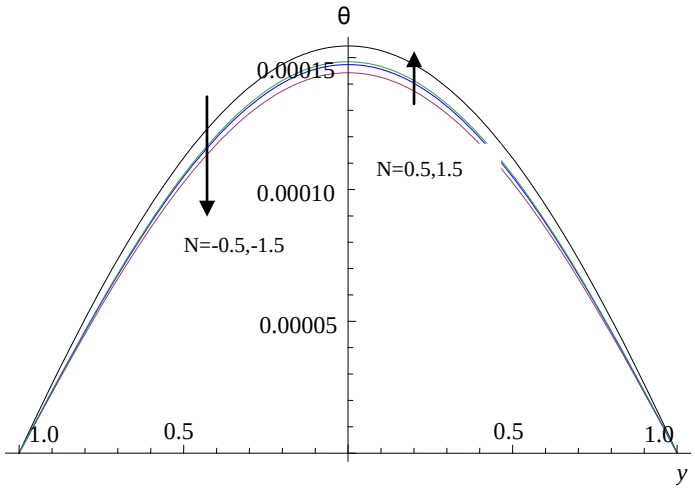

Figure-5b: Variation of θ with N
G=2, M=2, D^{-1}=0.2, Sc=1.3,Ec=0.01, F=0.5,Sr=0.5, Pr=0.71.

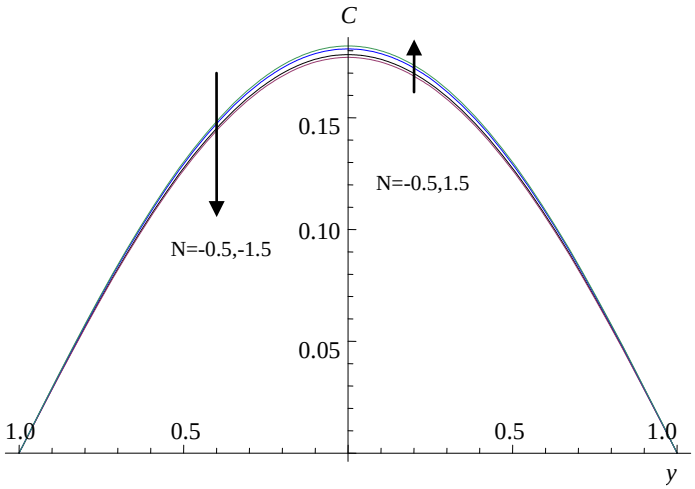

Figure-5c: Variation of C with N
G=2, M=2, D^{-1}=0.2, Sc=1.3, Ec=0.01, F=0.5, Sr=0.5, Pr=0.71.

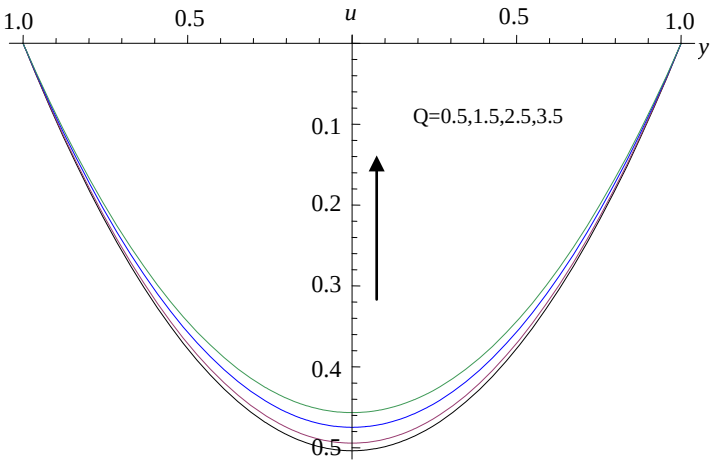

Figure-6a: Variation of u with Q>0
G=2, M=2, D^{-1}=0.2, N=1, Ec=0.01, Sc=1.3, Sr=0.5, Pr=0.71, F=0.5.

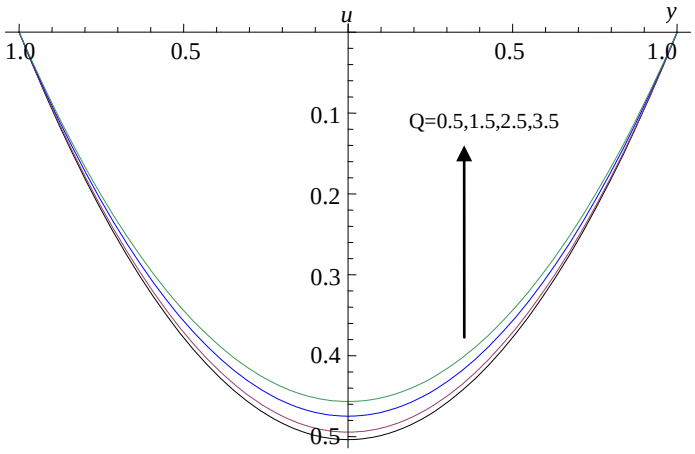

Figure-6b: Variation of θ with Q>0
G=2, M=2, D^{-1}=0.2, N=1, Ec=0.01, Sc=1.3, Sr=0.5, Pr=0.71, F=0.5.

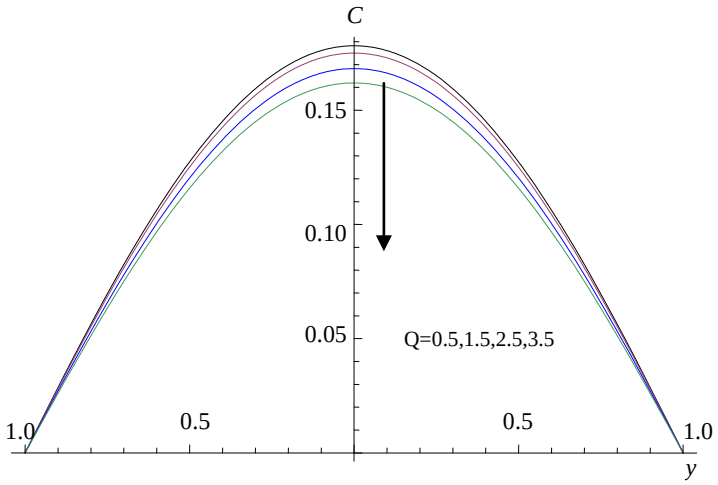

Figure-6c: Variation of C with Q>0
G=2, M=2, D^{-1}=0.2, N=1, Ec=0.01, Sc=1.3, Sr=0.5, Pr=0.71, F=0.5.

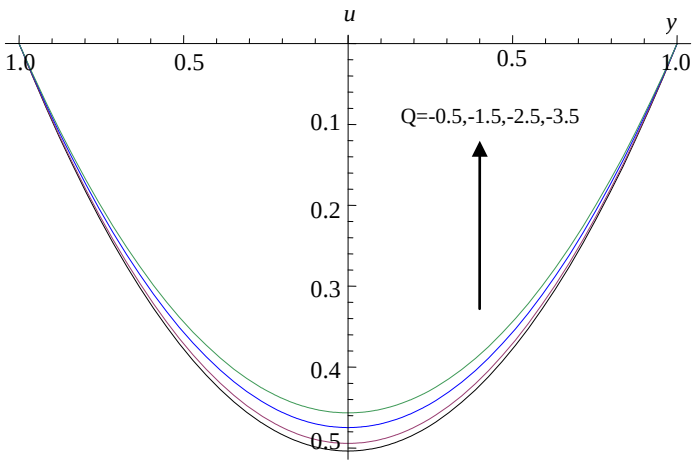

Figure-7a: Variation of u with Q<0
G=2, M=2, D^{-1}=0.2, N=1, Ec=0.01, S c=1.3, Sr=0.5, Pr=0.71, F=0.5.

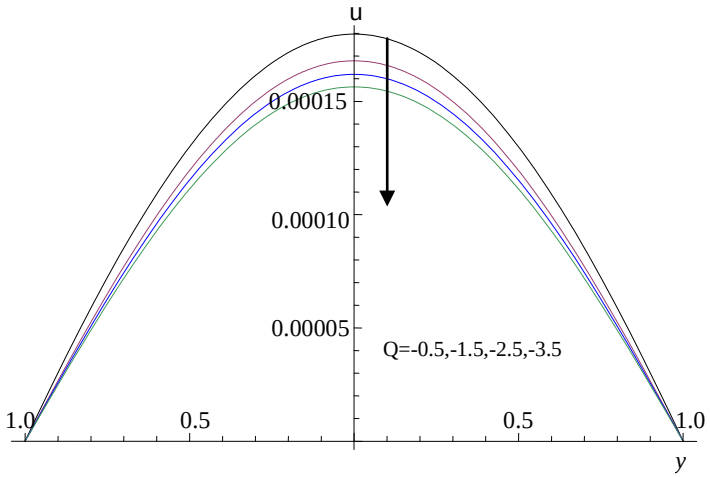

Figure-7b: Variation of u with Q<0
G=2, M=2, D^{-1}=0.2, N=1, Ec=0.01, Sc=1.3, Sr=0.5, Pr=0.71, F=0.5.

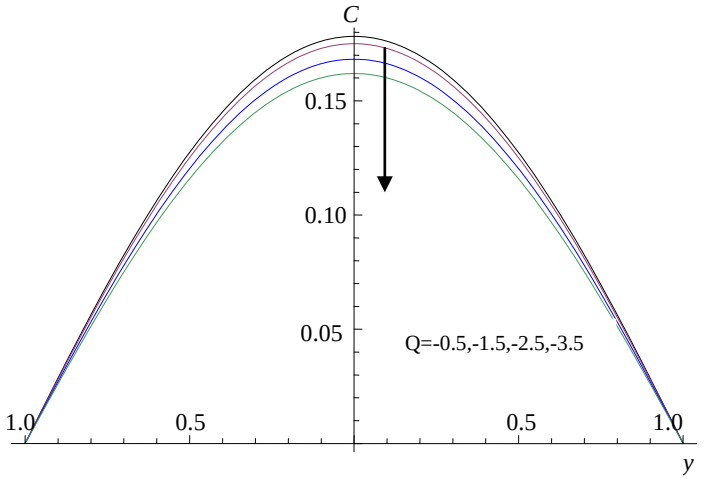

Figure-7c: Variation of u with Q<0
G=2, M=2, D^{-1}=0.2, N=1, Ec=0.01, Sc=1.3, Sr=0.5, Pr=0.71, F=0.5.

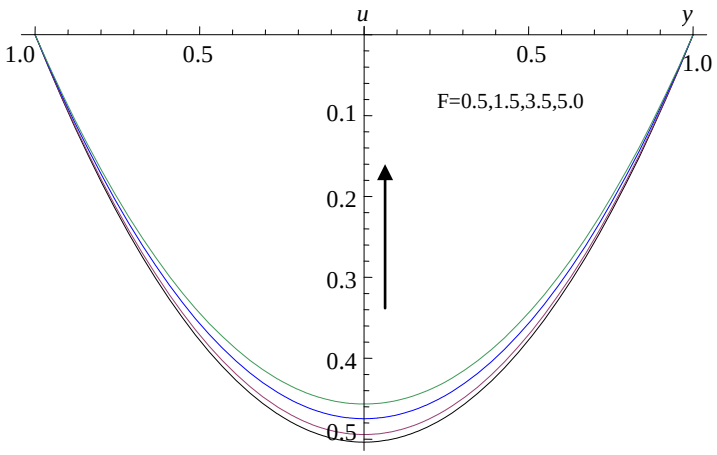

Figure-8a: Variation of u with F
G=2, M=2, D^{-1}=0.2, N=1, Ec=0.01, Sc=1.3, Sr=0.5, Pr=0.71.

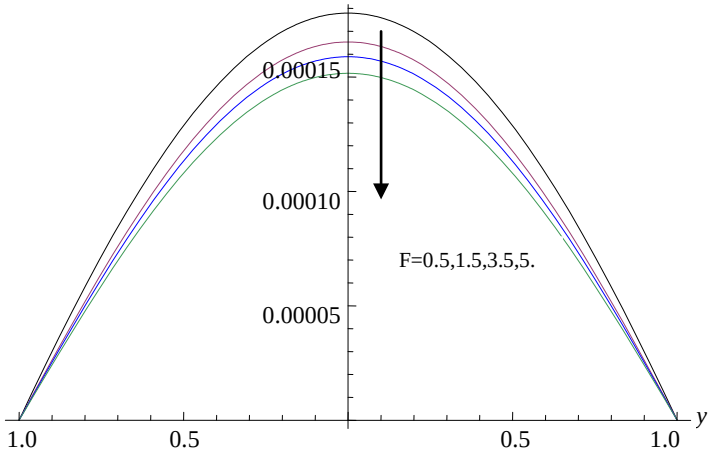

Figure-8b: Variation of θ with F
G=2, M=2, D^{-1}=0.2, N=1, Ec=0.01, Sc=1.3, Sr=0.5, Pr=0.71.

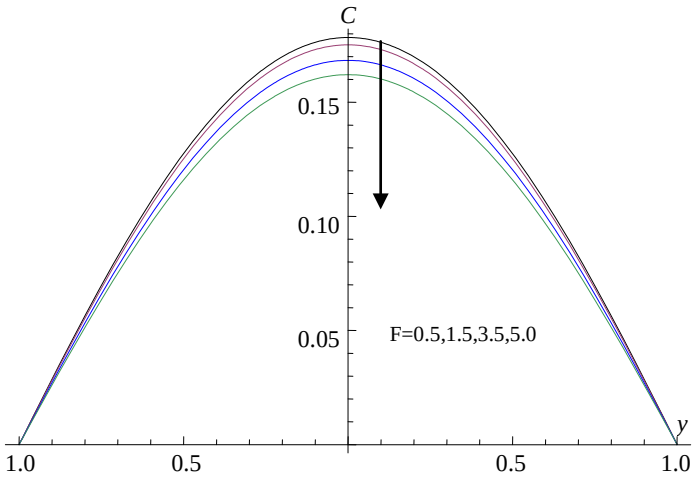

Figure-8c: Variation of C with F
G=2, M=2, D^{-1}=0.2, N=1, Ec=0.01, Sc=1.3, Sr=0.5, Pr=0.71

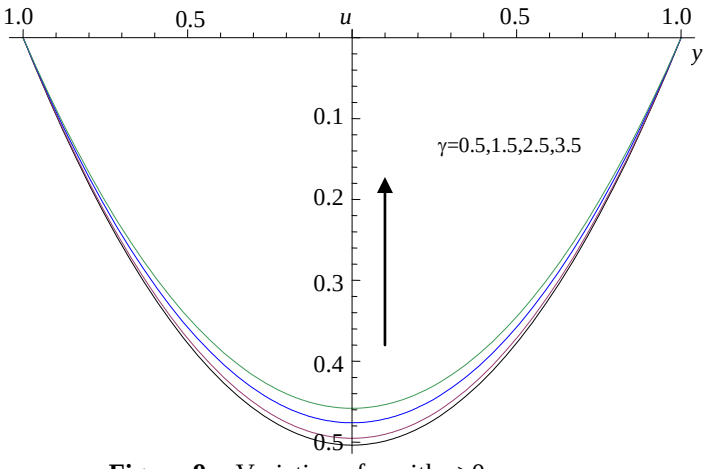

Figure-9a: Variation of u with γ>0
G=2, M=2, D^{-1}=0.2, N=1, Ec=0.01, Sc=1.3, Sr=0.5, Pr=0.71, F=0.5.

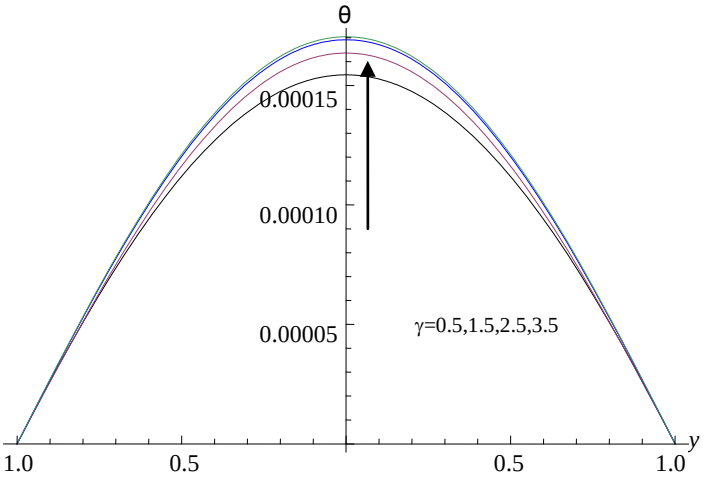

Figure-9b: Variation of θ with γ>0
G=2, M=2, D^{-1}=0.2, N=1, Ec=0.01, Sc=1.3, Sr=0.5, Pr=0.71, F=0.5.

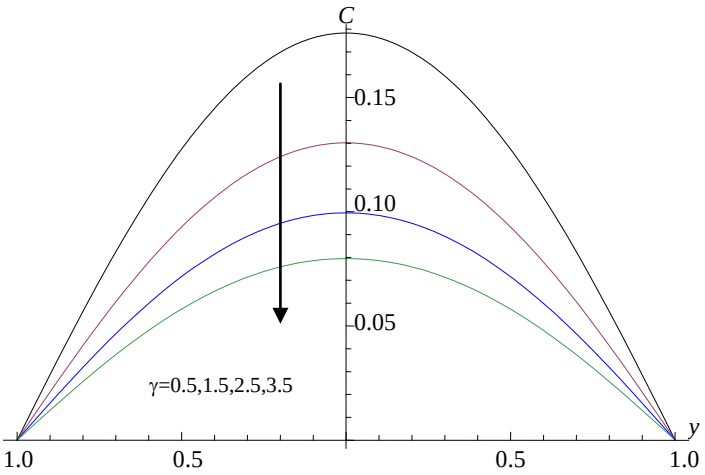

Figure-9c: Variation of C with γ>0
G=2, M=2, D^{-1}=0.2, N=1, Ec=0.01, Sc=1.3, Sr=0.5, Pr=0.71, F=0.5

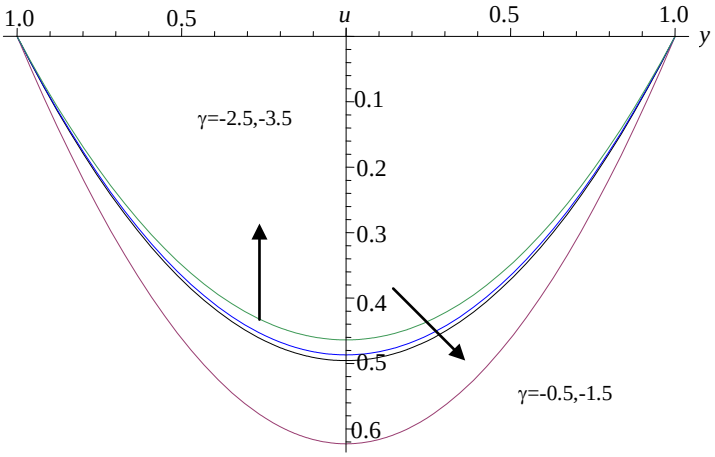

Figure-10a: Variation of u with γ<0, G=2,
M=2, D^{-1}=0.2, N=1, Ec=0.01, Sc=1.3, Sr=0.5, Pr=0.71, F=0.5

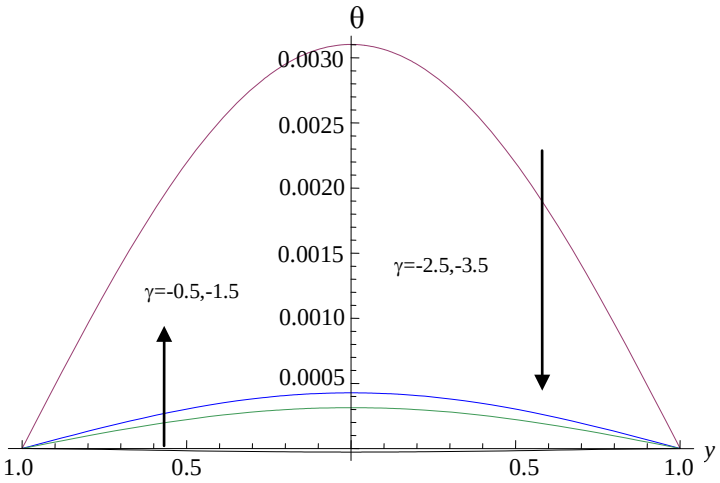

Figure-10b: Variation of u with γ<0,
G=2,.M=2, D^{-1}=0.2, N=1, Ec=0.01, Sc=1.3, Sr=0.5, Pr=0.71, F=0.5

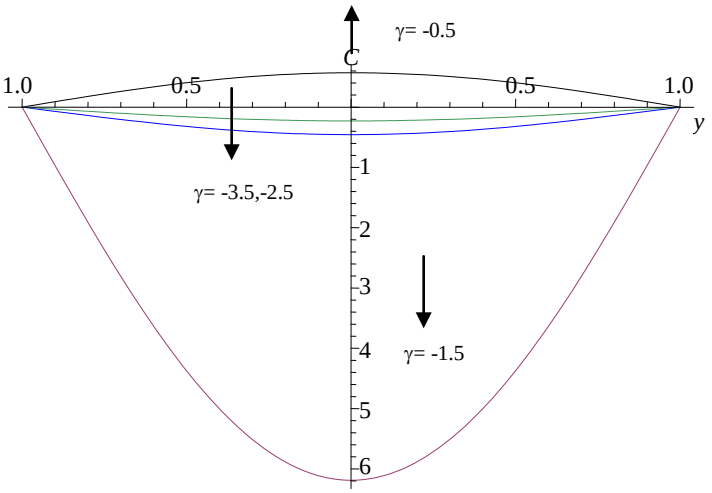

Figure-10c: Variation of C with γ < 0,
G=2, M=2, D^{-1}=0.2, N=1, Ec=0.01, Sc=1.3, Sr=0.5, Pr=0.71, F=0.5

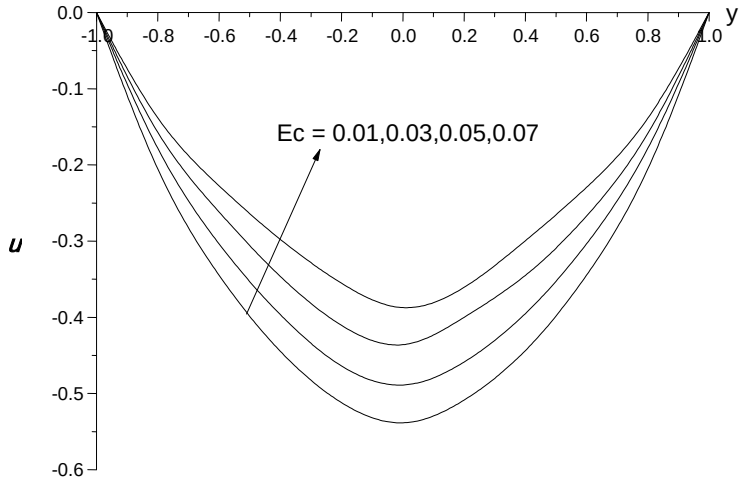

Figure-11a: Variation of u with Ec,
G=2, M=2, D^{-1}=0.2, N=1, γ=0.5, Sc=1.3, Sr=0.5, Pr=0.71, F=0.5, Q=0.5

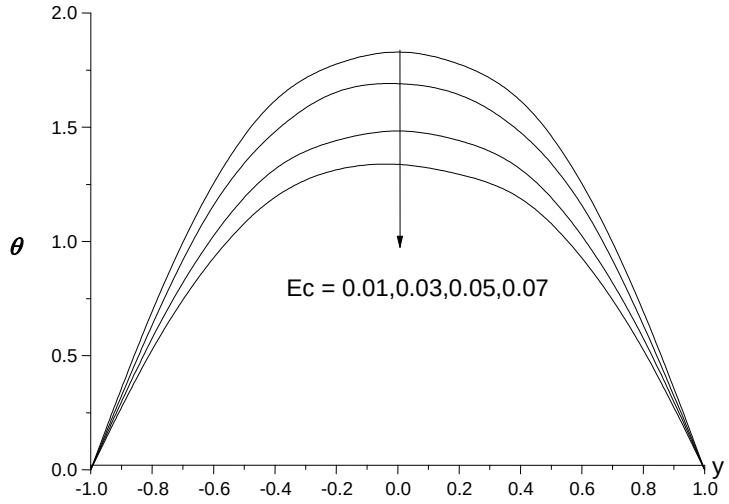

Figure-11b: Variation of θ with Ec,
G=2, M=2, D^{-1}=0.2, N=1, γ=0.5, Sc=1.3, Sr=0.5, Pr=0.71, F=0.5, Q=0.5

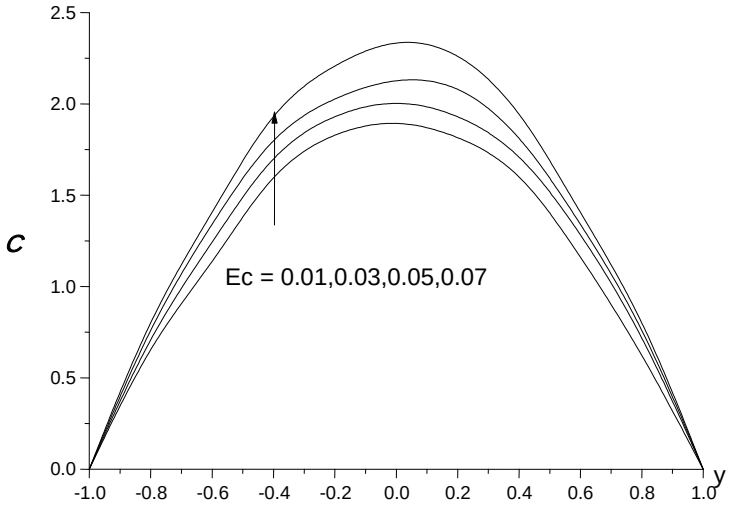

Figure-11c: Variation of C with Ec,
G=2, M=2, D^{-1}=0.2, N=1, γ=0.5, Sc=1.3, Sr=0.5, Pr=0.71, F=0.5, Q=0.5

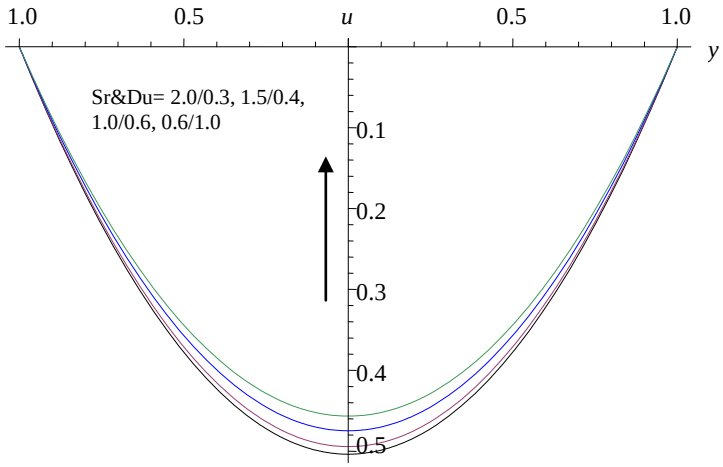

Figure-12a: Variation of u with Sr & Du,
G=2, M=2, D^{-1}=0.2, N=1, γ=0.5, Sc=1.3, Ec=0.01, Pr=0.71, F=0.5, Q=0.5

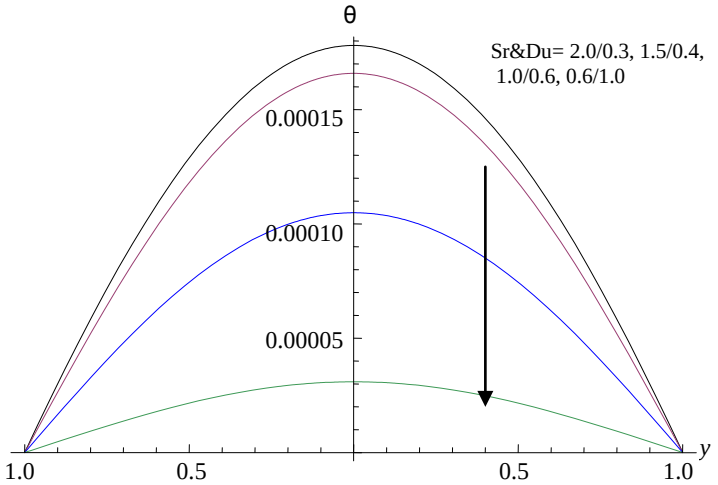

Figure-12b: Variation of θ with Sr & Du
G=2,.M=2, D^{-1}=0.2, N=1, γ=0.5, Sc=1.3, Ec=0.01, Pr=0.71, F=0.5, Q=0.5

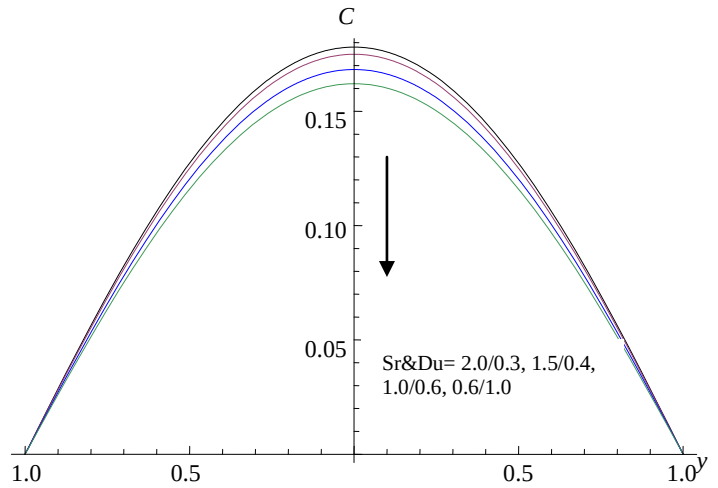

Figure-12c: Variation of C with Sr and Du
G=2, M=2, D^{-1}=0.2, N=1, γ=0.5, Sc=1.3, Ec=0.01, Pr=0.71, F=0.5, Q=0.5

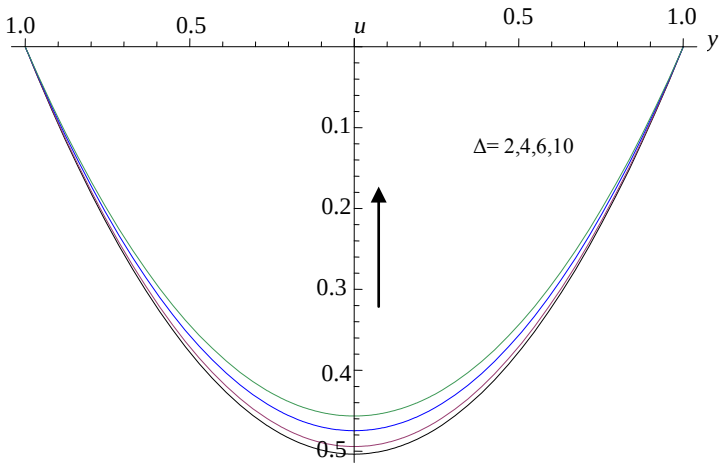

Figure-13a: Variation of u with Δ
G=2, M=2, D^{-1}=0.2, N=1, γ=0.5, Sc=1.3, Ec=0.01, Pr=0.71, F=0.5, Q=0.5, Sr=0.5

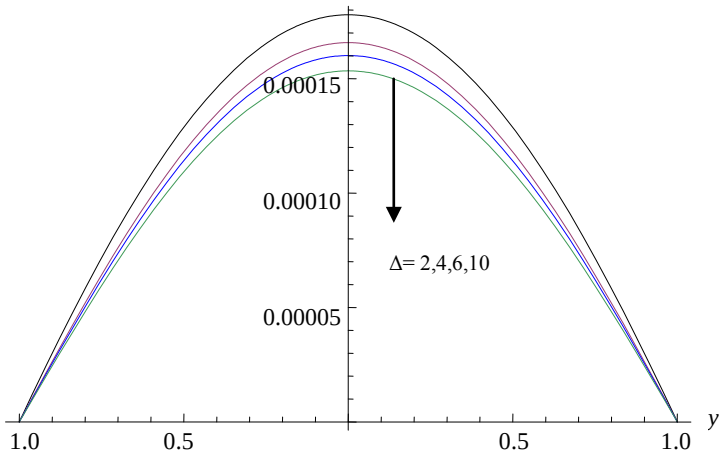

Figure-13b: Variation of θ with Δ
G=2, M=2, D^{-1}=0.2, N=1, γ=0.5, Sc=1.3, Ec=0.01, Pr=0.71, F=0.5, Q=0.5, Sr=0.5

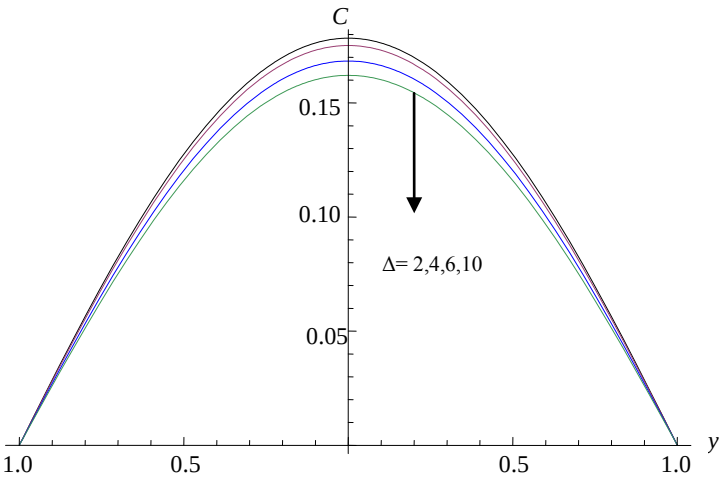

Figure-13c: Variation of C with Δ
G=2,.M=2, D^{-1}=0.2, N=1, γ=0.5, Sc=1.3, Ec=0.01, Pr=0.71, F=0.5, Q=0.5, Sr=0.5

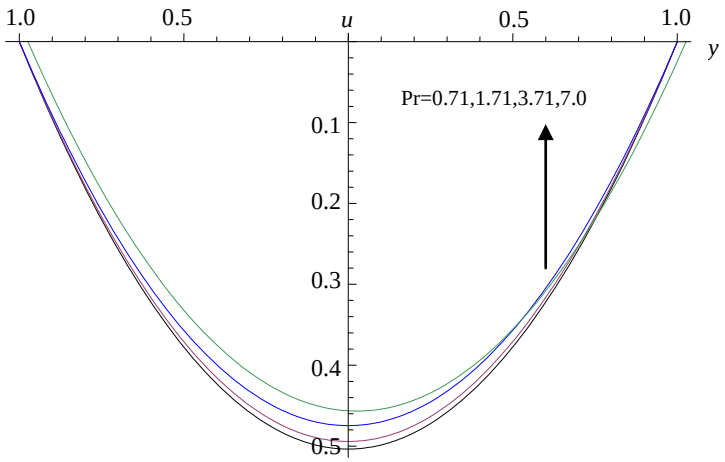

Figure-14a: Variation of u with Pr
G=2,.M=2, D^{-1}=0.2, N=1, γ=0.5, Sc=1.3, Ec=0.01, A=0.5, F=0.5, Q=0.5, Sr=0.5

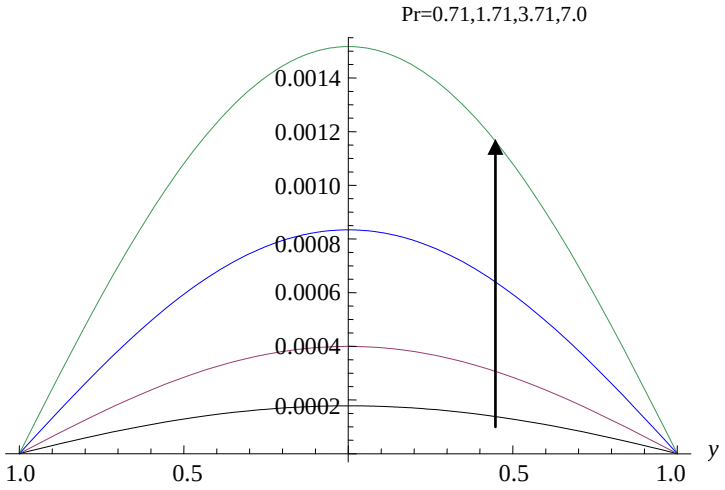

Figure-14b: Variation of θ with Pr

G=2, M=2, D^{-1}=0.2, N=1, γ=0.5, Sc=1.3, Ec=0.01, A=0.5, F=0.5, Q=0.5, Sr=0.5

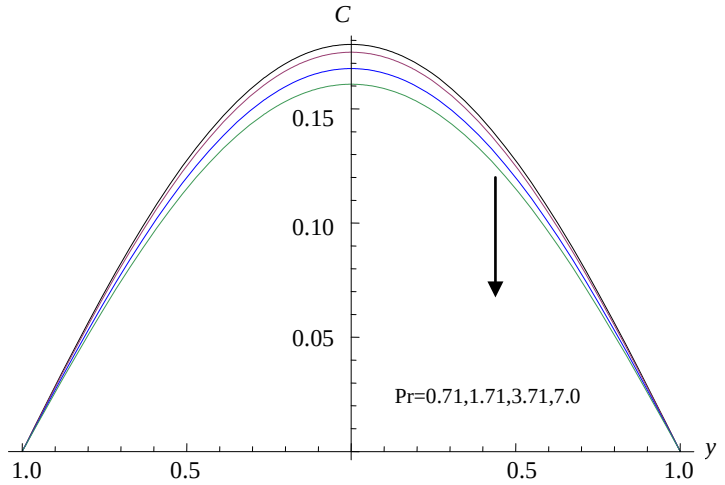

Figure-14c: Variation of C with Pr

G=2, M=2, D^{-1}=0.2, N=1, γ=0.5, Sc=1.3, Ec=0.01, A=0.5, F=0.5, Q=0.5, Sr=0.5

Table-1: Skin Friction (τ), Nusselt Number (Nu) and Sherwood Number at y=±1

Parameter		τ(-1)	τ(+1)	Nu(-1)	Nu(+1)	Sh(-1)	Sh(+1)
G	10	-1.00603	1.00603	-0.306088	0.306088	-0.287423	0.287423
	20	-1.00218	1.00218	-0.283527	0.283527	-0.287932	0.287932
	30	-0.99466	0.99466	-0.265742	0.265742	-0.283551	0.283551
	50	-0.98909	0.98909	-0.355186	0.355186	-0.281556	0.281556
M	0.5	-1.00603	1.00603	-0.306088	0.306088	-0.287423	0.287423
	1.0	-1.04971	1.04971	-0.29971	0.29971	-0.252343	0.252343
	1.5	-1.13027	1.13027	-0.309473	0.309473	-0.329838	0.329838
	2.0	-1.27384	1.27384	-0.478628	0.478628	-0.378818	0.378818
D-1	0.2	-1.00603	1.00603	-0.306088	0.306088	-0.287423	0.287423
	0.4	-1.0036	1.0036	-0.28403	0.28403	-0.239213	0.239213
	0.6	-0.99932	0.99932	-0.267282	0.267282	-0.285178	0.285178
	0.8	-0.996006	0.99600	-0.358254	0.358254	-0.283971	0.283971
N	1.0	-1.00603	1.00603	-0.306088	0.306088	-0.287423	0.287423
	2.0	-1.00218	1.00218	-0.283529	0.283529	-0.238795	0.238795
	-0.5	-1.01771	1.01771	-0.273242	0.273242	-0.291483	0.291483
	-1.5	-1.02367	1.02367	-0.370293	0.370293	-0.293452	0.293452
Q	2	-1.00603	1.00603	-0.306968	0.306968	-0.287423	0.287423
	4	-1.00698	1.00698	-0.285177	0.285177	-0.240174	0.240174
	-2	-1.00603	1.00603	-0.271928	0.271928	-0.287461	0.287461
	-4	-1.00599	1.00599	-0.367054	0.367054	-0.287379	0.287379
Sc	0.24	-1.01033	1.01033	-0.37755	0.37755	-0.073819	0.0738193
	0.66	-1.00827	1.00827	-0.30662	0.30662	-0.175717	0.175717
	1.3	-1.00603	1.00603	-0.26944	0.26944	-0.287463	0.287463
	2.01	-1.00432	1.00432	-0.36182	0.36182	-0.374325	0.374325

γ	0.5	-1.00603	1.00603	-0.306088	0.306088	-0.287423	0.287423
	1.5	-1.00751	1.00751	-0.293456	0.293456	-0.215333	0.215333
	-0.5	-0.993421	0.993421	-0. 064958	0.064958	-0.901586	0.901586
	-1.5	-1.21905	1.21905	-0.0455824	0.0455822	-1.007586	1.007586
F	0.5	-1.00603	1.00603	-0.184107	0.1841072	-0.287531	0.287531
	1.5	-1.00559	1.00559	-0.089981	0.0899801	-0.287617	0.287617
	3.5	-1.00459	1.00459	-0.047483	0.474835	-0.287653	0.287653
	5.0	-1.00395	1.00395	-0.047108	0.471084	-0.287659	0.287659
Ec	0.01	-1.00603	1.00603	-0.184107	0.184107	-0.287531	0.287531
	0.03	-1.00613	1.00613	-0.0162061	0.162061	-0.287555	0.287555
	0.05	-1.00625	1.00625	-0.162043	0.162043	-0.287561	0.287561
	0.07	-1.00644	1.00644	-0.218107	0.218107	-0.287571	0.287571
Sr/Du	2.0/0.3	-1.00603	1.00603	-0.184139	0.184139	-0.28787	0.28787
	1.5/0.4	-1.00653	1.00653	-0.193391	0.193391	-0.28771	0.28771
	1.0/0.6	-1.00753	1.00753	-0.205996	0.205996	-0.28763	0.28763
	0.6/1.0	-1.00853	1.00853	-0.218765	0.218765	-0.16292	0.16292
Δ	2	-1.00603	1.00603	-0.184139	0.184139	-0.28737	0.287372
	4	-1.00599	1.00599	-0.62089	0.162089	-0.28741	0.287417
	6	-1.00588	1.00588	-0.62086	0.162086	-0.28745	0.287452
	10	-1.00459	1.00459	-0.161875	0.168754	-0.28854	0.288544
Pr	0.71	-1.00603	1.00603	-0.306088	0.306088	-0.287423	0.287423
	1.71	-1.00697	1.00697	-0.687057	0.687057	-0.239886	0.239886
	3.71	-1.00603	1.00603	-0.1409572	0.1409572	-0.286485	0.286485
	7.0	-1.00602	1.00602	-0.3574723	0.3574723	-0.287462	0.287627

CONCLUSIONS

The non-linear coupled equations governing the flow have solved by employing Galerkin finite element technique. The effect of Soret effect, dissipation ,radiation on all the flow characteristics have displayed graphically. The conclusions of this analysis are:

1) An increase in Grashof number reduces the velocity, temperatutre, concentration and Skin friction on the walls.The Nusselt number reduces and the Sherwood number enhances with $G \leq 20$ and for higher $G \geq 30$, a reversed effect is noticed on Nu and Sh.
2) The velocity reduces, the temperature, concentration and Skin friction enhances with increasing M. An increase in $M \leq 4$ reduces Nu ans Sh and for higher $M \geq 6$, they enhance on the walls.
3) An increase in D-1 reduces the velocity, enhances the temperature, skin friction on the walls and concentration. An increase in $D\text{-}1 \leq 0.4$ reduces the Nusselt nu7mber and She4rwood nu7mber and for higher $D\text{-}1 \geq 0.6$,we notice an enhancement o Nu and Sh on the walls.
4) Lesser the molecular diffusivity smaller the velocity, temperature, skin friction and larger the concentration and Sherwood number. An increase in $Sc \leq 1.3$ reduces Nu and enhances Nu with higher $Sc \geq 2.01$.
5) The velocity, temperature, concentration, Skinfriction, Nusselt number and Sherwood number reduce withy increase in the buoyancy ratio $N>0$ and for $N<0$, except temperature all flow variables enhance in the flow region.
6) An increase in the strength of the heat generating source enhances the velocity, skin friction, reduces the Nusselt number and for $Q<0$, the velocity, Skin friction reduce and the Nusselt number enhance on the walls. The temperature, concentration, and Sherwood number reduce with increase in the strength of the heat generating/absorbing source.
7) Higher the radiative heat flux lesser the velocity, temperature, concentration, skin friction, Nusselt number and larger the Sherwood number on the walls.
8) The velocity, temperature and concentration, Nusselt number and Sherwood number reduce, skin friction enhances in the degenerating chemical reaction case. In the generating chemical reaction case, the velocity, temperature enhances, the concentration reduces with increase in $|\gamma| \leq 1.5$ and for higher $|\gamma| \geq 2.5$, we notice a reversed effect on them. The skin friction, Nusselt number and Sherwood number enhance on the both walls.
9) Higher the dissipative effects smaller the axial velocity, larger the actual temperature and concentration. The skin friction and Sherwood number enhance on the wall with Ec. The Nusselt number reduces with $Ec \leq 0.05$ and enhances with higher $Ec \geq 0.07$.
10) Increasing Sr (or decreasing Du) enhances the velocity, temperatrure and Sherwood number, while the the concentration, Skin friction, Nusselt number reduce on the walls.
11) Increase in Fochhemeir number Δ reduces the velocity, concentration, skin friction, Nusselt nulber while the temperature and Sherwood number increases.
12) The velocity, concentration reduce, the temperature and Nusselt number enhances with increase in Pr. An increase in $Pr \leq 1.71$, enhances the Skin friction and reduces the Sherwood number while for higher $Pr \geq 3.71$, we notice ereduction in Skin friction and enhancement in Sh.

7. REFERENCES

1. Abdual Sattar.M.D, Hamid Kalim.M.D: Unsteady free-convection interaction with thermal radiation in a boundary layer flow past a vertical porous plate. J Math Phys Sci; 30:25-37 (1996).
2. Adrian Postelnicu : Influence of magnetic field on heat and mass transfer by natural convection from vertical surfaces in porous media considering Soret and Dufour effects. Int. J. of Heat and Mass Transfer, V.47, pp.1467-1472 (2004).
3. Alam, M.S., Rahman, M.M., Abdul Maleque M. (2005). Local Similarity solutions for unsteady MHD free convention and mass transfer flow past an impulsively started vertical porous plate with Dufour and Soret effects. *ThammasatInt J Sci Tech* 10, 1-18.
4. Alam, M.S., Rahman, M.M., Samad M A (2006). Dufour and Soret effects on unsteady MHD free convection and mass transfer flow past a vertical porous plate in a porous medium. *Non-linear Anal Modell Contr*,11, 217-26.
5. Al-Nimir, M.A,Haddad,O.H, Fully developed free convection in open-ended vertical chasnnels partially filled with porous material,J.Porous Media ,V.2,pp.179-189(1999).
6. Alam, Md, Delower Hossain, M and Arif Hossain, M: Viscous dissipation and joule heating effects on steady MHD combined heat and mass transfer flow through a porous medium in a rotating system. Journal of Naval Architecture and Marine Engineering, V.2, pp.105-120 (2011).
7. Bakier A.Y and Gorla R.S.R., Thermal radiation effects on mixed convection from horizontal surfaces in porous media Transport in porous media, Vol.23 pp 357-362 (1996).
8. Barletta, A: Laminar mixed convection with viscous dissipation in a vertical channel. Int. J. Heat Mass Transfer, V.41, PP.3501-3513 (1998).
9. Barletta,A., Analysis of combined forced and free flow in a vertrical channel with viscous dissipation and isothermal-isoflux boundary conditions, ASME. J. Heat Transfer ,V,121, pp.349-356(1999).
10. Barletta,A,Magyari,E and Kellaer,B., Dual mixed convection flows in a vertical channel.,INny.J.Heat and Mass Transfer,V.48,pp.4835-4845(2005).
11. Barletta,A,Celli,M and Magtyari,E and Zanchini,E., Buoyany MHD flows in a vertical channel:the levitation regime.,Heat and Mass Transfer ,V.44,pp.1005-1013(2007).
12. Beckermann,C.Visakanta,r and.Ramadhyani,S., A numerical study of non-Darcian natural convection in a vertical enclosure filled with a porous medium., Numerical Heat transfer 10, pp.557-570, (1986).
13. Brewester,M.Q., Thermal radiative transfer properties.,John Wiley and Sons (1972)
14. Cebeci,T,Khattab,A.A and LaMont,R., Combined natural and forced convection in a vertical ducts,in:Proc.7th Int. Heat Transfer Conf.,V.3,pp.419-424(1982).
15. Chamkha A.J., Solar Radiation Assisted natural convection in a uniform porous medium supported by a vertical heat plate, ASME Journal of heat transfer, V.19, pp 89-96 (1997).
16. Cheng, Heat transfer in geothermal systems. Adv. Heat transfer 14,1-105(1978).
17. Ching-Yang-Cheng (2011). Soret and Dufour effects on free convective boundary layer over inclined wavy surface in a porous medium. *Int. Communications in Heat and Mass Transfer* 38, 1050-1055.
18. Datta,N anfd Jana,R.N., Effect of wall conductance on hydromagnetic convection of a radiation gas in a vertical channel., Int.J.Heat Mass Transfer,V.19,pp.1015-1019(1974).
19. Deepti,J, Prasada Rao,D.R.V., Finite element analysis of chemically reaction effect on Non-Darcy convective heat and mass transfer flow through a porous medium in a vertical channel with constant heat sources.,Int.J.Math.Arch,V.3(11), pp.3885-3897(2012).
20. Dulal Pal and Sewli Chatterjee., Heat and Mass transfer in MHD non-Darcian flow of a micropolar fluid over a stretching sheet embedded in a porous media with non-uniform heat source and thermal radiation, Communications in Nonlinear Science and Numerical Simulation, Volume 15, Issue 7, Pages 1843-1857 (2010).
21. Dulal Pal and Babulal Talukdar., Perturbation analysis of unsteady magneto hydro dynamic convective heat and mass transfer in a boundary layer slip flow past a vertical permeable plate with thermal radiation and chemical reaction, Communications in Nonlinear Science and Numerical Simulation, Volume 15, Issue 7, July 2010, P.1813-1830 (2010).
22. Dulal pal, Hiranmoy Mondal (2011). Effect of Soret, Dufour, chemical reaction and thermal radiation on MHD,non-darcy, unsteady mixed convective heat and mass transfer over stretching sheet. *Common Non-linear Sci Numer Simulat* 16, 1942-1958.
23. Dulal pal, Hiranmoy Mondal (2012). Effects on MHD non-darcian mixed convective heat and mass transfer over a stretching sheet with non-uniform heat source/sink. *Physica B* 407 642-651.
24. Gebhart, B.J., Effects of viscous dissipation in natural convection", fluid Mech, V.14,pp.225 -232 (1962).
25. Gebhert,B and Mollendorf: J., Viscous dissipation in external natural convection flows Fluid Mech,V.38, pp.97-107(1969).
26. Gill,W.N and Del Casal,A., A theoretical investigation of natural convection effects in a forced horizontal flows,AIChE J,V.8,pp.513-518(1962).
27. Greif, R, Habib, I.S and Lin,J.c., Laminar convection of a radiating gas in a vertical channel, J.Fluid. Mech., V.46, p.513(1971).

28. Gupta,P.S and Gupta,A.S., Radiation effect on hydromagnetic convection in a vertical channel.,Int.J.heat Mass Transfer,V.127,pp.1437-1442(1973).
29. Jafarunnisa, S: Transient double diffusive flow of a viscous fluid with radiation effect in channels/Ducts, Ph.D Thesis, S.K.University, Anantapur, India (2011).
30. Indudhar Reddy, M, Narasimha Rao, P and Prasada Rao, D.R.V: Effect of Quadratic density-temperature variation on unsteady convective heat and mass transfer flow in a vertical channel. J. Pure & Appl. Phys., V.23, No.2, pp.175-187 (2011).
31. Kalidas.N. and Prasad, V., Benard convection in porous media Effects of Darcy and Pransdtl Numbers, Int. Syms. Convection in porous media, non-Darcy effects, proc.25th Nat. Heat Transfer Conf.V.1, pp.593-604 (1988).
32. Kamalakar,P.V.S Prasada Rao,D.R.V and Raghavendra Rao,R., Finite element analysis of chemical reaction effect on Non-Darcy convective heat and mass transfer flow through a porous medium in a vertical channel with heat sources., Int.J.Appl.Math and Mech,V,8(13), pp.13-28(2012).
33. Kafoussias N G, Williams EW (1995). Thermal-diffusion and diffusion-thermo effects on mixed free-force convective and mass transfer boundary layer flow with temperature dependent viscosity. *Int J EngSci*33, 1369-84.
34. Laurait,G and.Prasad,V., Natural convection in a vertical porous cavity a numerical study of Brinkman extended Darcy formulation., J.Heat Transfer.pp.295-320(1987).
35. Lakshminarayan P A, Sibanda, (2010). Soret and Dufour effects on free convection along vertical wavy surface in a fluid saturated darcy porous medium.*Int. J. of Heat and Mass Transfer* 53, 3030-3034.
36. Madhusudhan Reddy, Y, Prasada Rao, D.R.V: Effect of thermo diffusion and chemical reaction on non-darcy convective heat & mass transfer flow in a vertical channel with radiation. IJMA, V.4, pp.1-13 (2012).
37. Makinde OD., Free convection flow with thermal radiation and mass transfer past moving vertical porous plate. Int Comm Heat Mass Transfer; 32:1411-9 (2005).
38. Mosa.M.F., Radiative heat transfer in horizontal MHD channel flow with buoyancy effects and axial temperature gradient, Ph D thesis, Mathematics Dept, Bradford University, England, UK (1979).
39. Muthucumaraswamy, R , Dhanasekhar, N and Eswar Prasad, G : Rotation effects on flow past an accelerated isothermal vertical plate with chemical reaction of first order. IJMA, V.3, No.5, pp.2122-2129 (2012).
40. Nath.O, Ojha. S.N and Takhar. H.S., A study of stellar point explosion in a radiative MHD medium Astrophysics and space science, V.183, pp 135-145 (1991).
41. Naga Radhika V, Prasad Rao D R V (2010). Dissipative and radiation effects on heat transfer flow of a viscous fluid in a vertical channel. *J. of Pure and Applied Phy.* 22(2), 255- 267.
42. Ostrach,S., Combined natural and forced convection laminar flow and heat transfer of fluid with and without heat sources in channels with linearly varying wall temperature, NACA TN,3141(1954).
43. Prasad, V.and Tuntomo, A.., Inertia Effects on Natural Convection in a vertical porous cavity, numerical Heat Transfer, V.11, pp.295-320 (1987).
44. Prasad.V, F.A,Kulacki and M.Keyhani;" Natural convection in a porous medium" J.Fluid Mech.150 p.89-119(`1985).
45. Poulikakos D., and Bejan, A.., The Departure from Darcy flow in Nat. Convection in a vertical porous layer, physics fluids V.28, pp.3477-3484 (1985).
46. Rajasekhar, N.S, Prasad, P.M.V and Prasada Rao, D.R.V: Effect of Hall current, Thermal radiation and thermo diffusion on convective heat and mass transfer flow of a viscous, rotating fluid past a vertical porous plate embedded in a porous medium. Advances in Applied Science Research, V.3, No.6, pp.3438-3447 (2012).
47. Rajesh, V and Varma.S.V.K., Radiation effects on MHD flow through a porous medium with variable temperature or variable mass diffusion, Int.J. of Appl.Math and Mech.6(1).p.39-57 (2010).
48. Raptis, A.A., Radiation and free convection flow through a porous medium, Int. commun. Heat and mass transfer, Vol. 25, pp 289-295 (1998).
49. Ravidra,M and Ramakrishna,G N: Effect of dissipation and thermal radiation on non-darcy mixed convective heat and mass transfer flow in a vertical channel.,Presented in NICT Conference,Dec,16&17(2016), S.S.B.N.Degree College, Anantapuramu, India
50. Raju, C.S.K, Sandeep, N., Sulochana, C., Sugunamma, V., Jayachandra Babu, M. (2015). Radiation, Inclined Magnetic field and Cross-Diffusion effects on flow over a stretching surface. *Journal of Nigerian Mathematical Society (In Press)*
51. Raju, C.S.K., Sandeep, N., Jayachandra Babu,M., Sugunamma, V., (2015). Radiation and chemical reaction effects on thermophoretic MHD flow over an aligned isothermal permeable surface with heat source.
52. Raju, C. S. K., Jayachandra Babu, M., Sandeep, N., Sugunamma, V., Reddy, J.V.R (2015). Radiation and soret effects of MHD nanofluid flow over a moving vertical plate in porous medium, *Chemical and ProcessEngineering Research* 30, 9-23.
53. Ramana Reddy, J.V., Sugunamma,V., Sandeep, N., Mohan Krishna, P. (2014). Thermal diffusion and chemical reaction effects on unsteady MHD dusty viscous flow. *Advances in Physics Theories and Applications*38, 7-21.

54. Shatevi, S., Thermal Radiation and Buoyancy Effects on Heat and Mass Transfer over a Semi-Infinite stretching surface with Suction and Blowing , journal of Applied mathematics,v.2008,Article id.414830,12pages (2008).
55. Sreevani M., Mixed convective heat and mass transfer through a porous medium in channels with dissipative effects, Ph.D thesis, S.K.University, Anantapur, India (2003).
56. Soundelgekar, V.M and Pop, I : Viscous dissipation effects on unsteady free convective flow past an infinite vertical porous plate with variable suction. Int. J. Heat mass transfer, V.17, pp.85-92 (1974).
57. Sulochana.c, Tayappa.H: Finite element analysis of thermo-diffusion and diffusion- thermo effects on combined heat and mass transfer flow of viscous, electrically conducting fluid through a porous medium in vertical channel, Int . J. mathematical achieves – 5(9), 2014, PP: 1-13.
58. Tao,L.N., On combined and forced convection in channels, ASME J.Heat Transfer, V.82, pp.233-238(1960).
59. Tien, D., and Hong, J.T., Natural convection in porous media under non-Darcian and non-uniform permeability conditions, hemisphere, Washington. (1985).
60. Tong, T.L and Subramanian, E., A boundary layer analysis for natural correction in porous enclosures: use of the Brinkman-extended Darcy model, Int.J.Heat Mass Transfer.28, pp.563-571 (1985).
61. Umadevi,B,Sreenivas,G,Bhuvana vijaya,R and prasada Rao,D.R.V., Finite element analysis of chemical reaction effect on Non-Darcy mixed convective double diffusive heat transfer flow through a porous medium in a vertical channel with constant heat sources., Adv. Appl. Sci. Res. V.3 (5), pp.2924-2939(2012).
62. Vafai, K., Tien, C.L., Boundary and Inertia effects on flow and Heat Transfer in Porous Media, Int. J. Heat Mass Transfer, V.24. Pp.195-203 (1981).
63. Vafai, K., Thyagaraju, R., Analysis of flow and heat Transfer at the interface region of a porous medium, Int. J. Heat Mass Trans., V.30pp.1391-1405 (1987).
64. Wirtz,R.A and McKinley,P.,Buoyancy effects on downward laminar convection between parallel plates.Fundamental of forced and mixed convection, ASME HTD,V.42,pp.105-112(1985).
65. Zanchini E., Effect of viscous dissipation on mixed convection in a vertical channel with boundary conditions of the third kind, Int. J. Heat mass transfer, V.41, pp.3949-3959 (1998).

Source of support: Nil, Conflict of interest: None Declared.